Ioffe Institute



Peter Shternin

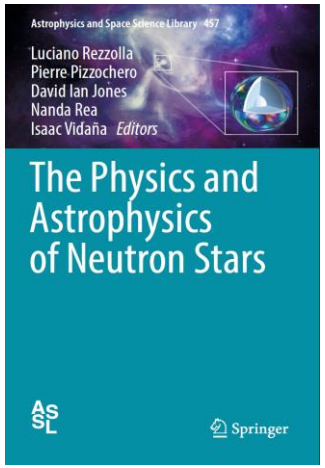
Transport theory of neutron star matter

(microphysical input)

Schmitt A., Shternin P. (2018). Chapter IX in: Rezzolla L., Pizzochero P., Jones D., Rea N., Vidaña I. (eds) The Physics and Astrophysics of Neutron Stars. ASSL, vol 457, Springer

Dr. Andreas Schmitt
University of Southampton





General remarks on transport

Transport: transfer of conserved quantities (energy, momentum, particle number, electric charge, corona virus…) from one region to another due to non-equilibrium conditions (temperature gradient, non-uniform chemical composition, ...)



- transport properties usually computed from quasiparticle collisions: energy & momentum exchange or flavor-changing processes (quasiparticle picture is not valid in strong coupling)
- in NS mostly degenerate matter (small $T \ll \mu$). Transport is dominated by fermions (electrons, muons, neutrons, protons, hyperons, quarks, neutrinos)
- if fermion contribution is suppressed (e.g. by Cooper pairing), bosons may dominate (lattice phonons, superfluid phonons, pions,…)

Astrophysical manifestations/phenomenology

Phenomenon	Transport properties
oscillatory modes (r-modes)	shear & bulk viscosities
pulsar glitches	superfluid transport
thermal radiation	heat transport in outermost layers
cooling	neutrino emissivity, thermal conductivity
magnetic field evolution	magnetohydrodynamics, electrical & thermal conductivities, reaction rates
crust disruption (accretion, magnetar flares, X-ray bursts)	transport properties of the crust, crustal nuclear transmutations (deep crustal heating)
core-collapse supernovae	neutrino transport
neutron star mergers	high-temperature transport, viscous MHD

many weird things happens at the graveyard



Basic transport coefficients-1

Boltzmann equation (example: non-relativistic, single species)

$$\frac{\partial f}{\partial t} + \boldsymbol{u} \cdot \frac{\partial f}{\partial \boldsymbol{x}} + \boldsymbol{R} \cdot \frac{\partial f}{\partial \boldsymbol{p}} = I[f]$$

Multiply by conserved quantities 1, $\boldsymbol{p}$, $\frac{p^2}{2m}$, and integrate over $\boldsymbol{p}$ → hydrodynamic eqs

$$\frac{\partial \rho}{\partial t} + \nabla \cdot \rho \boldsymbol{v} = 0$$

continuity equation

$$\frac{\partial s}{\partial t} + \nabla \cdot \left(s\boldsymbol{v} + \frac{\boldsymbol{j}_T}{T} \right) = -\frac{\pi_{ji}\partial_j v_i + \boldsymbol{j}_T \cdot \nabla T/T}{T}$$

entropy production

$$\frac{\partial v_i}{\partial t} + (\boldsymbol{v} \cdot \nabla) v_i = -\frac{\partial_i P}{\rho} + \frac{R_i}{m} - \frac{\partial_j \pi_{ji}}{\rho}$$

Navier-Stokes equation

Dissipative terms:

$$\boldsymbol{j}_T = -\kappa \nabla T$$

$$\pi_{ij} = -2\eta \left(v_{ij} - \frac{\delta_{ij}}{3} \nabla \cdot \boldsymbol{v} \right) - \zeta \delta_{ij} \nabla \cdot \boldsymbol{v}$$

with thermal conductivity κ, shear viscosity η, bulk viscosity ζ

Basic transport coefficients-2

General phenomenological approach:
add dissipative terms order by order in derivatives

$$T^{\mu\nu} = T^{\mu\nu}_{\rm eq} + \Delta T^{\mu\nu}(\partial, u, \varepsilon) = (\varepsilon + P)u^\mu u^\nu - P g^{\mu\nu} + q^\mu u^\nu + q^\nu u^\mu + \tau^{\mu\nu}$$

$$j^\mu = n u^\mu + J^\mu$$

$$J^\mu,\ q^\mu,\ \tau^{\mu\nu} = \mathcal{O}(\partial) + \mathcal{O}(\partial^2) + \dots$$

Use conservation equations to derive dissipative hydrodynamics

$$\partial_\mu T^{\mu\nu} = 0, \quad \partial_\mu j^\mu = 0$$

General recipe:
obtain transport coefficients from microscopic theory (e.g., from Boltzmann equation) and use in hydrodynamic equations

Going to neutron star conditions

- General relativistic effects

$$p^\mu \frac{\partial f}{\partial x^\mu} - \Gamma^\mu{}_{\nu\rho}\, p^\nu p^\rho \frac{\partial f}{\partial p^\mu} = I[f]$$

Important for neutrino transport

Mean free paths are small $l \ll R$; can work in proper frame and introduce GR at the end

Example: heat flux

$$F_r = -\kappa\, e^{-\lambda-\phi} \frac{\partial \tilde{T}}{\partial r}$$

Exceptions: large l: neutrinos, superfluid phonons,…

- Collective (mean field) effects: Fermi-liquid theory, plasma effects (self-consistent electromagnetic field, screening).

- Multifluid transport (mixtures), in particular
- Superfluid transport → more transport coefficients, non-trivial topology (e.g. vortices, fluxtubes)

Zoo of the transport properties in NSs

$M \sim 1 - 2 M_\odot$

$R \sim 12$ km

Good things: small T, usually strong degeneracy, everything happens on Fermi surfaces

Bad things: many processes and phases, largely unknown

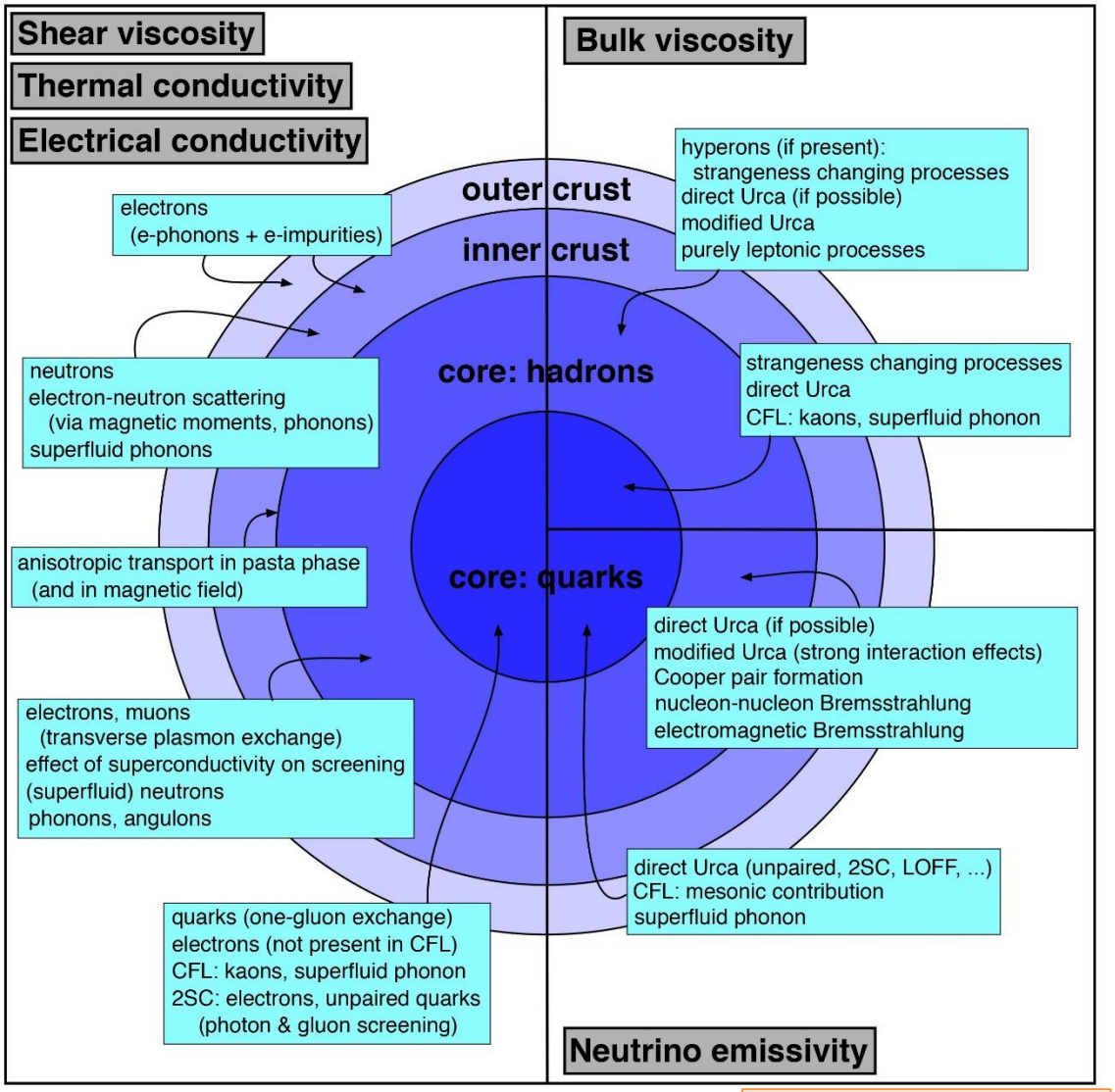


figure by Andreas Schmitt

Rest of the talk

Part I. Transport in NS core and crust

- **Shear viscosity and thermal conductivity in NS cores. Uncertainty from many-body nuclear theory.**
- **Non-FL behavior of electromagnetic collisions in relativistic plasma. Role of plasma screening.**
- **Transport in NS crusts. Crustal cooling in quasi-persistent LMXBs**

Part II

- **Neutrino emission in NSs and NS cooling.**
- **Low-energy theorem for electroweak bremsstrahlung emission. MUrca `enhancement' in beta-stable nuclear matter**

Part III

- **Bulk viscosity in NS cores**

Contents

Part I: Transport coefficients in NS core and crust

a) NS core
b) NS crust

Astro: Young NS cooling

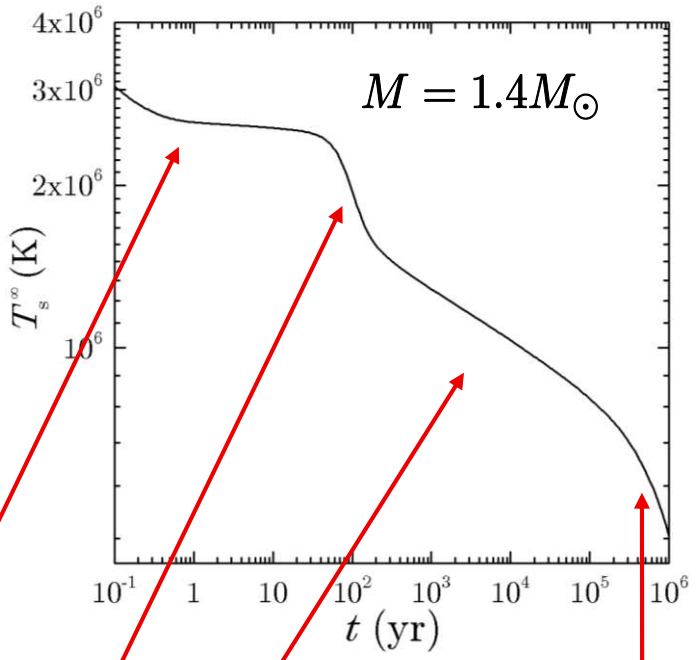
$$C\frac{\partial \widetilde{T}}{\partial t} + \nabla \cdot (\mathrm{e}^{\Phi} F) = \mathrm{e}^{2\Phi} Q_\nu$$

$$F = -\mathrm{e}^{-\Phi}\hat{\kappa}\nabla\widetilde{T}$$

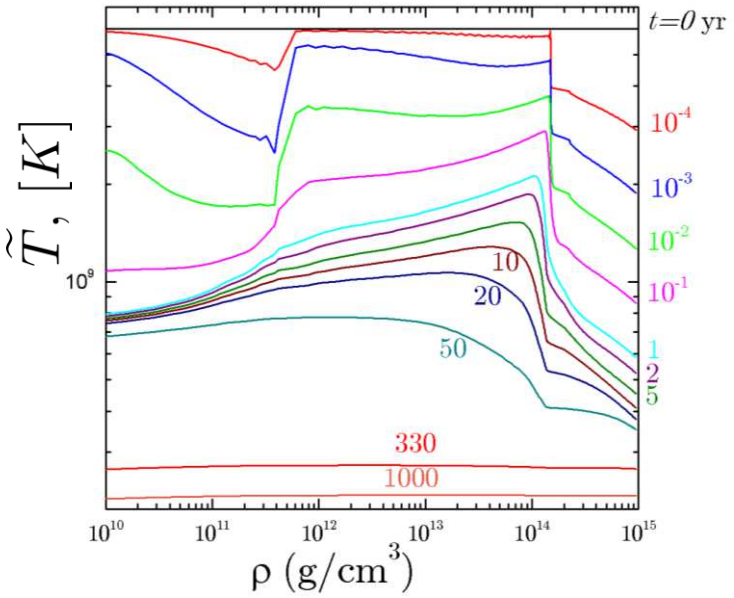
redshifted internal temperature

$$\widetilde{T} = \mathrm{e}^{\Phi} T$$

Typical cooling curve



internal temperature



Crustal cooling

Relaxation

$t_r \sim 30 - 300$ yr

Neutrino stage

Photon stage

$$C\frac{\mathrm{d}\widetilde{T}}{\mathrm{d}t} = -L_\nu^\infty - L_\gamma^\infty + L_{\mathrm{heat}}$$

Thermal conductivity impacts early cooling stages. Determine duration of relaxation (crustal κ more important, though)

wait for next talks

Astro: r-modes and GW emission

Oscillation r-modes (restoring force - Coriolis) in rotating stars are unstable to GW emission. NSs in binaries are spun up by accretion to the instability window, where unstable grow of r-modes results in fast heating and spindown, quickly returning sources to stable region. However, many sources in instability window are observed

Stability criterion for r-modes

$$\frac{1}{\tau_{GW}(f)} + \frac{1}{\tau_{\zeta}(f,T)} + \frac{1}{\tau_{\eta}(T)} > 0$$

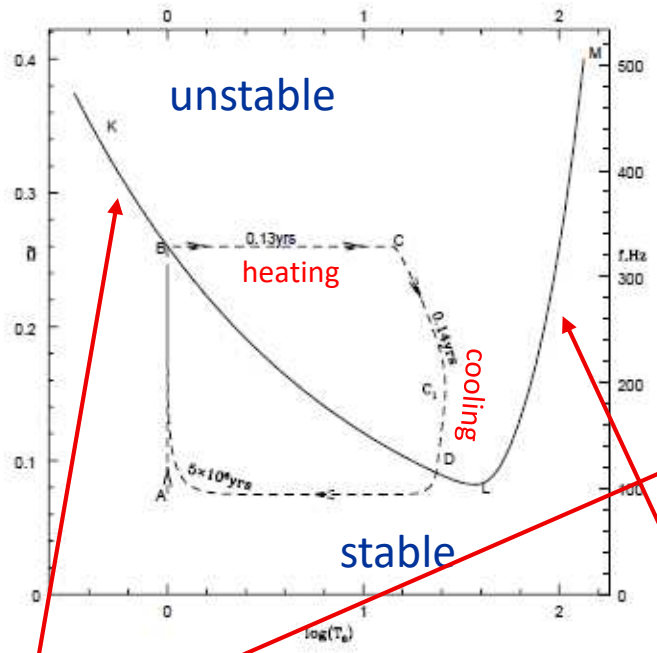


figure from *Levin, ApJ 517, 328 (1999)*

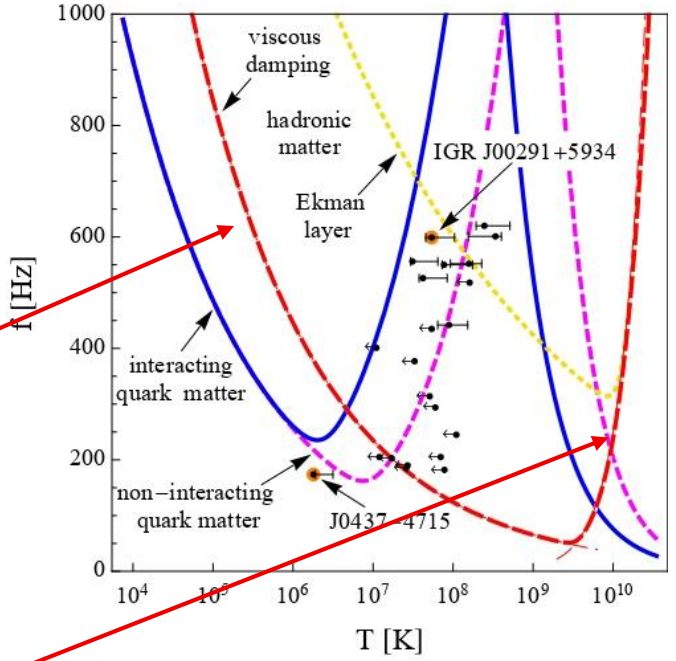


figure from *Alford, Schwenzer, PRL 113, 1102 (2014)*

shear viscosity damping

bulk viscosity damping

Diffusive transport coefficients. Relaxation time

small deviations from equilibrium: linear theory
linearization of transport equation (Chapman-Enskog method)

$$f(\boldsymbol{x},\boldsymbol{u},t) \approx f^{(0)} + \delta f\,, \qquad \delta f = -\frac{\partial f^{(0)}}{\partial \varepsilon}\Phi + \mathcal{O}(\Phi^2) \approx \frac{f^{(0)}(1-f^{(0)})}{k_B T}\Phi$$

I.e. Fermi-Dirac function

$$\frac{\partial f^{(0)}}{\partial t} + \boldsymbol{u}\cdot\frac{\partial f^{(0)}}{\partial \boldsymbol{x}} + \boldsymbol{R}\cdot\frac{\partial f^{(0)}}{\partial \boldsymbol{p}} \approx I_{\rm lin}[\Phi]$$

$$f^{(0)}(\boldsymbol{x},\boldsymbol{u},t) = \left\{\exp\left[\frac{\varepsilon(\boldsymbol{x},\boldsymbol{u},t)-\mu(\boldsymbol{x},t)}{k_B T(\boldsymbol{x},t)}\right]+1\right\}^{-1}$$

solve to find Φ and obtain transport coefficient from the expressions for the fluxes

relaxation-time approximation (elastic collisions $\omega \ll k_B T$)

$$I[f] = -\sum_{lm}\frac{\delta f^{lm}}{\tau^l(\varepsilon)}Y_{lm}(\Omega_{\boldsymbol{p}})$$

example: thermal conductivity in r.t.a.

$$\nabla T \to -\frac{\varepsilon - h}{T}\boldsymbol{u}\cdot\nabla T\;\frac{\partial f^{(0)}}{\partial \varepsilon} = \frac{\partial f^{(0)}}{\partial \varepsilon}\frac{\Phi}{\tau^1(\varepsilon)} \quad \Rightarrow \quad \Phi = -\frac{\varepsilon - h}{T}\boldsymbol{u}\cdot\nabla T\;\tau^1(\varepsilon)$$

thermal flux in linear regime

$$\boldsymbol{j}_T = -\int_{\boldsymbol{p}}\Phi\frac{\partial f^{(0)}}{\partial \varepsilon}(\varepsilon - h)\boldsymbol{u} = -\frac{\pi^2 k_B^2 T n}{3m}\tau^1(\mu)\nabla T = -\kappa\nabla T$$

Multicomponent Fermi-liquid

collision of degenerate particles: r.t.a. does not work ($\omega \sim k_B T \ll p_{Fi}$)

$$I_{\rm lin}[\Phi] = -\frac{1}{(1+\delta_{ci})k_B T}\int_{\boldsymbol{p}_2}\int_{\boldsymbol{p}_1'}\int_{\boldsymbol{p}_2'} W_{ci}(\boldsymbol{p}_1,\boldsymbol{p}_2,\boldsymbol{p}_1',\boldsymbol{p}_2') f_1^{(0)} f_2^{(0)}(1-f_{1'}^{(0)})(1-f_{2'}^{(0)})(\Phi_1+\Phi_2-\Phi_1'-\Phi_2')$$

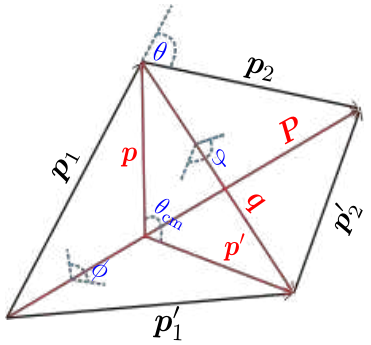
$$W_{ci}(\boldsymbol{p},\boldsymbol{p}_1,\boldsymbol{p}',\boldsymbol{p}_1') = \frac{2\pi^4}{\hbar}\delta(\epsilon_1+\epsilon_2-\epsilon_1'-\epsilon_2')\delta(\boldsymbol{P}-\boldsymbol{P}')\sum_{\rm spins}|M_{ci}|^2$$

Effective relaxation times (thermal conductivity & shear viscosity)

$$\kappa = \sum_c \frac{\pi^2 k_B^2 T n_c \tau_c^{\kappa}}{3 m_c^*}; \qquad \eta = \sum_c \frac{n_c p_{{\rm F}c}^2 \tau_c^{\eta}}{5 m_c^*}$$

$$\Phi^{\kappa,\eta} \to \tau_c^{\kappa,\eta} \to \kappa,\ \eta$$

$$1+2 \to 1'+2'$$



Variational solution /skip/

Kinetic equation

$$(\dot{F} =) X = I[\Phi]$$

Entropy generation rate

$$\int X\Phi = \int I[\Phi]\Phi = -T\varsigma \leq 0 \quad (*)$$

Variational principle: solution of the transport equation realizes maximal entropy generation among functions subject to constrain (*)

Example: thermal conductivity

$$T\varsigma = -j_T \frac{\nabla T}{T} = \kappa \frac{(\nabla T)^2}{T} \qquad \kappa^{Var} \leq \kappa$$

Simplest variational solution is enough in the NS condition

$$\Phi^{\kappa} \propto (\varepsilon - \mu)\boldsymbol{v}\frac{\nabla T}{T} \qquad \Phi^{\eta} \propto (v_\alpha p_\beta - \frac{1}{3}\delta_{\alpha\beta} vp)V_{\alpha\beta}$$

Fermi-systems allows for exact solutions

Brooker and Sykes, 1968; Hojgard Jensen et al., 1968
Fowers and Itoh, 1979; Anderson et al., 1987

Transport coefficients in multicomponent Fermi liquid

$$\kappa = \sum_c \frac{\pi^2 k_B^2 T n_c \tau_c^{\kappa}}{3 m_c^*}; \quad \eta = \sum_c \frac{n_c p_{\mathrm{F}c}^2 \tau_c^{\eta}}{5 m_c^*}$$

system of transport equations reduces to a system of linear equations (simplest var. sol.)

$$\sum_i \left(\nu_{ci}\tau_c + \nu'_{ci}\tau_i\right) = 1$$

Direct collisions **Exchange collisions**

effective collision frequencies are angular averages of collision probabilities

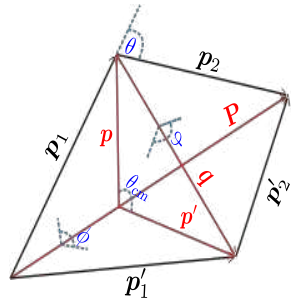
$$\nu_{ci} \propto \left\langle |M_{ci}|^2 W(\Omega) \right\rangle_\Omega$$

In Fermi-liquid limit $M \neq M(\varepsilon)$: collisions only reorient momenta on Fermi surface, then

$$\nu_{ci} \propto T^2 \qquad \kappa \propto T^{-1} \qquad \eta \propto T^{-2}$$

microphysical input

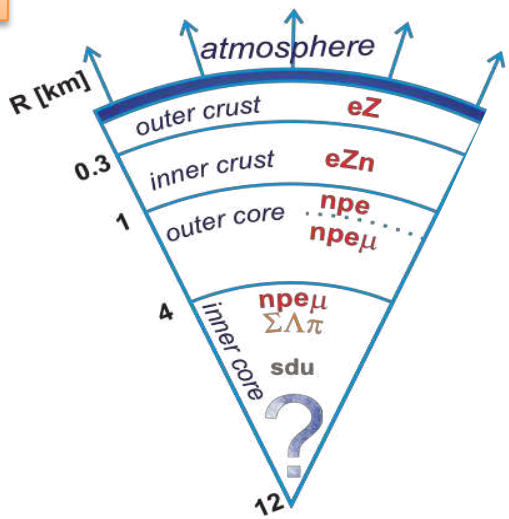
$$m^*, \ |M_{ci}|^2$$ on the Fermi surface



Transport in NS cores

Example: beta-stable npeμ matter

$$\mu_n = \mu_p + \mu_\ell$$



Decoupling in two sectors:

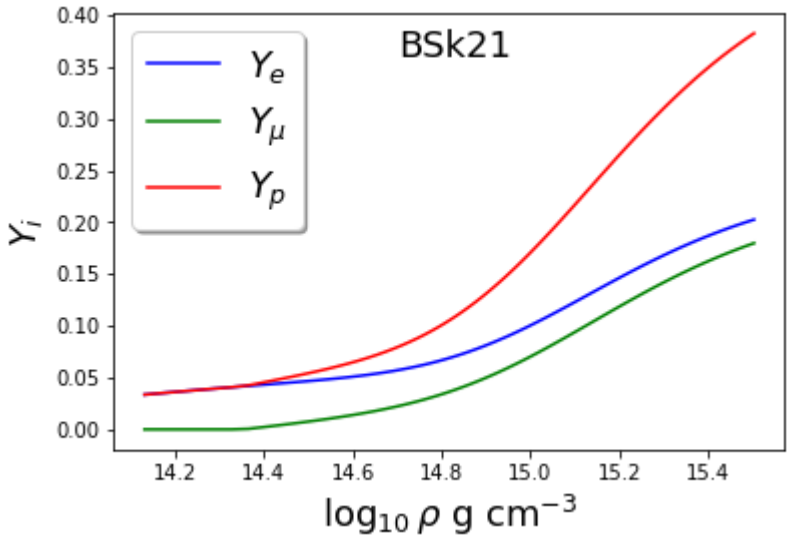
$$\kappa = \kappa_{e\mu}[ee, e\mu, ep] + \kappa_n[nn, np]$$

$$\kappa_{\rm p} \ll \kappa_{\rm n}$$

Electromagnetic sector $\kappa_{e\mu},\ \eta_{e\mu}$

Nuclear (strong interactions) sector $\kappa_{\rm n},\ \eta_{\rm n}$

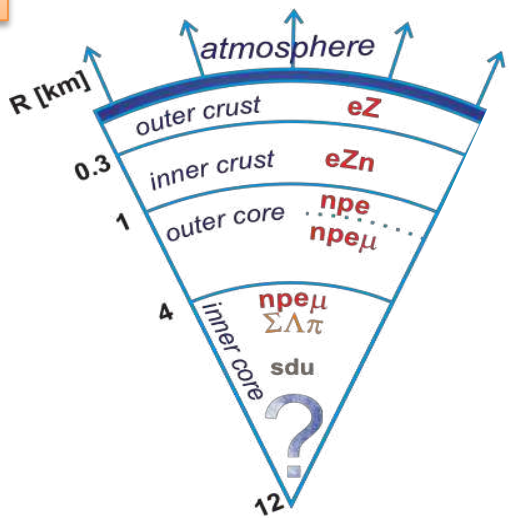
E. Flowers, N. Itoh, ApJ 230, 847 (1979)



Transport in NS cores

Example: beta-stable npeμ matter

$$\mu_n = \mu_p + \mu_\ell$$



Decoupling in two sectors:

$$\kappa = \kappa_{e\mu}[ee, e\mu, ep] + \kappa_n[nn, np]$$

$$\kappa_{\rm p} \ll \kappa_{\rm n}$$

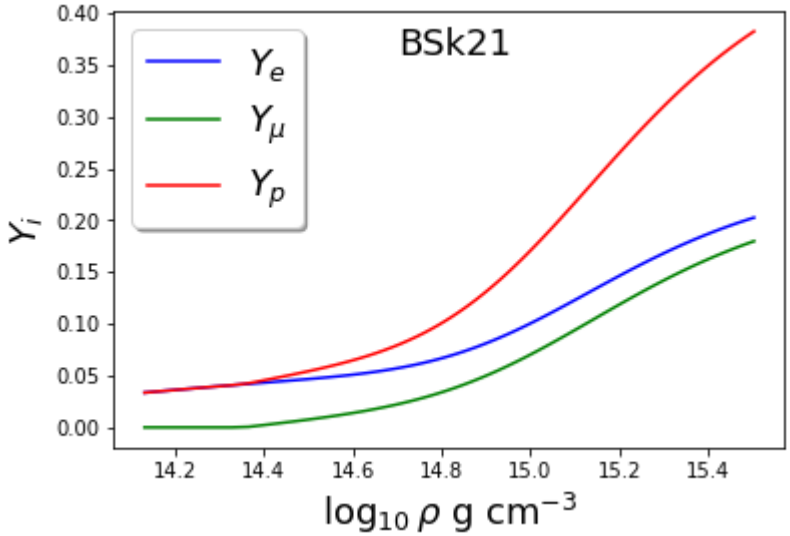
Electromagnetic sector $\kappa_{e\mu},\ \eta_{e\mu}$

Nuclear (strong interactions) sector $\kappa_{\rm n},\ \eta_{\rm n}$

E. Flowers, N. Itoh, ApJ 230, 847 (1979)

Need in-medium nucleon interaction in dense matter => many-body nuclear theory

Example: Brueckner-Hartree-Fock scheme



Brueckner-Hartree-Fock

Interaction is described via the in-medium scattering G-matrix

Start from 'realistic' nucleon potentials $\hat{V} \rightarrow \hat{G}$

$$\hat{G} = \hat{V} + \hat{V}\frac{\hat{Q}_{\rm Pauli}}{E - \hat{H}}\hat{G}$$

Bethe-Goldstone equation with the self-consistent potential

$$\langle p_1 p_2 | G^{\alpha\beta}(\omega) | p_3 p_4 \rangle = \langle p_1 p_2 | V^{\alpha\beta} | p_3 p_4 \rangle + \sum_{k_1,k_2} \langle p_1 p_2 | V^{\alpha\beta} | k_1 k_2 \rangle \frac{Q^{\alpha\beta}(k_1,k_2)}{\omega - \epsilon_\alpha(k_1) - \epsilon_\beta(k_2)} \langle k_1 k_2 | G^{\alpha\beta} | p_3 p_4 \rangle$$

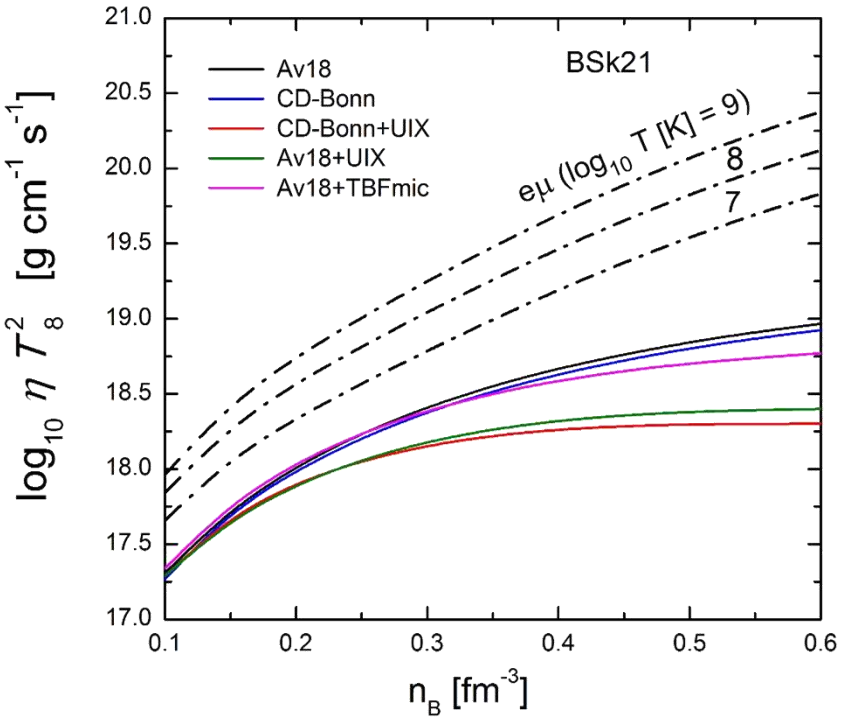
$$\epsilon_\alpha(p) = \frac{p^2}{2m_\alpha} + U_\alpha(p) \qquad U_\alpha(p_1) = \sum_{\beta; p_2 < p_{F\beta}} \langle p_1 p_2 | G^{\alpha\beta}(\epsilon_1(p_1) + \epsilon_2(p_2)) | p_1 p_2 \rangle_{\rm A}$$

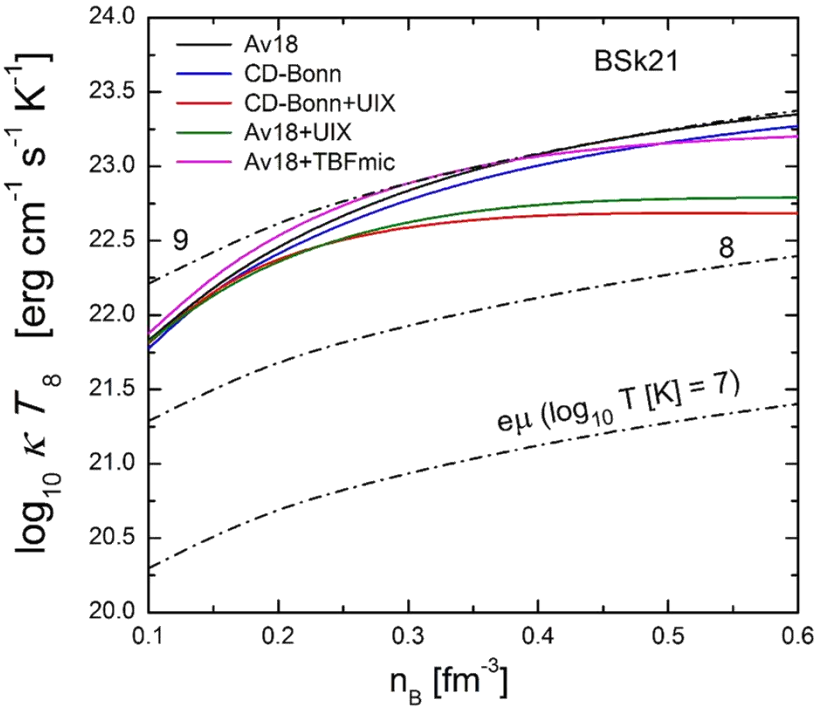
Three-body forces can be included in BHF scheme as effective two-body interaction

Neutron transport in Brueckner-Hartree-Fock

Example: two realistic NN potentials plus two three-body force models.
Only a single many-body approach, but large uncertainty at high n_B

$\eta_n \propto T^{-2}$ **Shear viscosity and thermal conductivity** $\kappa_n \propto T^{-1}$





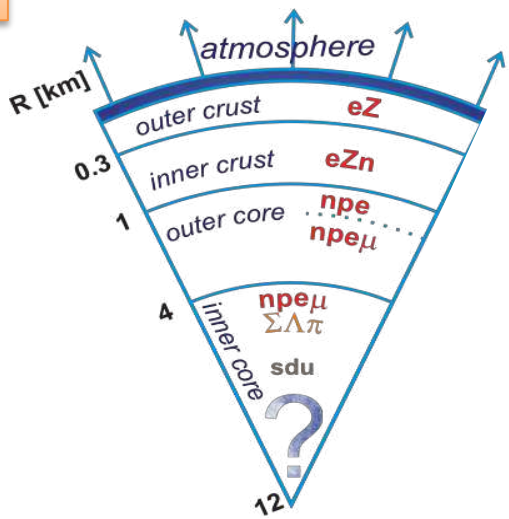
Why electromagnetic part behaves differently?

$n_0 = 0.16\ \mathrm{fm}^{-3}$
nuclear saturation density

Transport in NS cores

Example: beta-stable npeμ matter

$$\mu_n = \mu_p + \mu_\ell$$



Decoupling in two sectors:

$$\kappa = \kappa_{e\mu}[ee, e\mu, ep] + \kappa_n[nn, np]$$

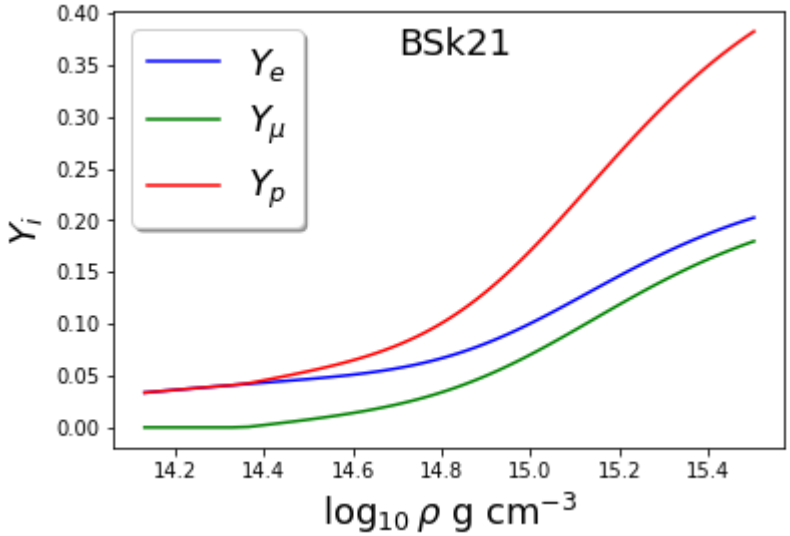
$$\kappa_{\rm p} \ll \kappa_{\rm n}$$

Electromagnetic sector $\kappa_{e\mu},\ \eta_{e\mu}$

Nuclear (strong interactions) sector $\kappa_{\rm n},\ \eta_{\rm n}$

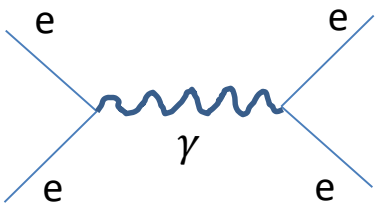
E. Flowers, N. Itoh, ApJ 230, 847 (1979)

Need in-medium modification of electromagnetic interaction (plasma screening)

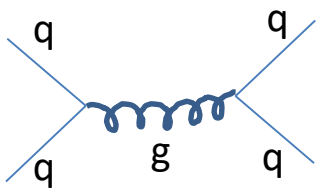


Electromagnetic collisions / quark collisions

nuclear matter:
ee (or $\mu\mu$) scattering (also NN)



quark matter:
qq scattering (also ee)



need photon (gluon) propagator in medium: screening

e.g., S. Stetina et al. PRC 97, 045801 (2018)

scattering in relativistic plasma is dominated by transverse plasmon exchange

H. Heiselberg, G. Baym, C.J. Pethick, and J. Popp, NPA 544, 569C (1992)

transverse plasmons screened dynamically via Landau damping

$$\eta_{ee} \propto \frac{1}{T^{5/3}} \sim 10^{20} \frac{\mathrm{g}}{\mathrm{cm\,s}}$$

$$\kappa_{ee} = \mathrm{const}(T) \sim 10^{22} \frac{\mathrm{erg}}{\mathrm{cm\,s\,K}}$$

Shternin & Yakovlev, PRD 74 043004 (2006); 75, 103004 (2007); 78, 063006 (2008)

non-FL behavior

$$\eta_{qq} \propto \frac{1}{T^{5/3}} \sim 10^{15} \frac{\mathrm{g}}{\mathrm{cm\,s}}$$

$$\kappa_{qq} = \mathrm{const}(T) \sim 10^{23} \frac{\mathrm{erg}}{\mathrm{cm\,s\,K}}$$

Heiselberg & Pethick, PRD 48, 2916 (1993)

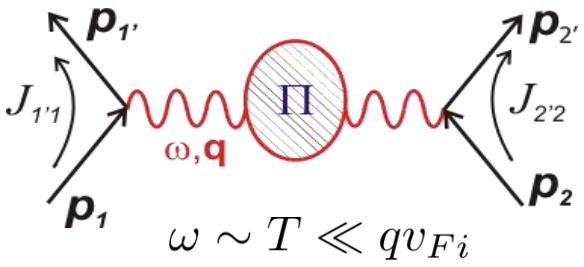
Plasma screening

Collision frequency due to electromagnetic interactions

$$\nu_{ci} = \tau_{ci}^{-1} \propto \left\langle |M_{ci}|^2 \, w_{tr}(q) \mathcal{F}_{\rm Pauli}(\omega) \right\rangle$$

Charged particles: Coulomb + Ampere (essentially relativisic $|\boldsymbol{J}_t|/J^{(0)} \propto v/c$)

$$M_{ci} = \frac{4\pi\hbar\alpha_f}{c}\left(\frac{J_1^{(0)} J_2^{(0)}}{q^2 + \Pi_l(\omega,q)} - \frac{\boldsymbol{J}_{1t}\cdot\boldsymbol{J}_{2t}}{q^2 - \omega^2 + \Pi_t(\omega,q)}\right)$$



$$\omega \sim T \ll q v_{Fi}$$

Everything is determined by the character of plasma screening

$$\Pi_l(\omega,q) = q_{\rm TF}^2 \qquad \Pi_t(\omega,q) = -i\frac{\pi}{4}\frac{\omega}{qc}q_t^2$$

Screening momentum is small ($q_{scr} \sim \omega^{1/3} \sim T^{1/3}$)
hence transverse channel dominates ($\nu_t \gg \nu_l$)

$$\nu_{ci} = \nu_{ci}^l + \nu_{ci}^t \qquad \nu_{ci}^l \propto T^2 \qquad \nu_{ci}^t \propto T^{2-\xi}$$

$$\kappa_{e\mu}^{t,N} = \frac{\pi^2}{54\zeta(3)}\frac{k_B c(p_{Fe}^2 + p_{Fp}^2)}{\hbar^2\alpha_f} \qquad \eta_{e\mu}^{t,N} = 1.1\frac{c^3\hbar^4}{\alpha_f}\frac{n_e^2 + n_\mu^2}{(\hbar c q_t)^{1/3}}(k_B T)^{-5/3}$$

Heiselberg & Pethick 1993

Shternin & Yakovlev 2007, 2008

Four screening regimes /skip/

Example: ee collisions in NS crust.

Regime	Electron velocity	Temperature	Main contribution	T-dependence of κ_{ee}
I	$v_e \ll c$	$T \gtrsim T_{pe}$	ν^l	$T^2/\ln(T/T_{pe})$
II	$v_e \ll c$	$T \ll T_{pe}$	ν^l	$1/T$
III	$v_e \approx c$	$T \gtrsim T_{pe}$	$\nu^l + \nu^t + \nu^{lt}$	$T^2/\ln(T/T_{pe})$
IV	$v_e \approx c$	$T \ll T_{pe}$	ν^t	const

$$T_{pe} = \frac{\hbar\omega_{pe}}{k_B} = \sqrt{\frac{4\pi\hbar^2 e^2 n_e}{k_B^2 m_e^*}}$$

cold catalyzed crust

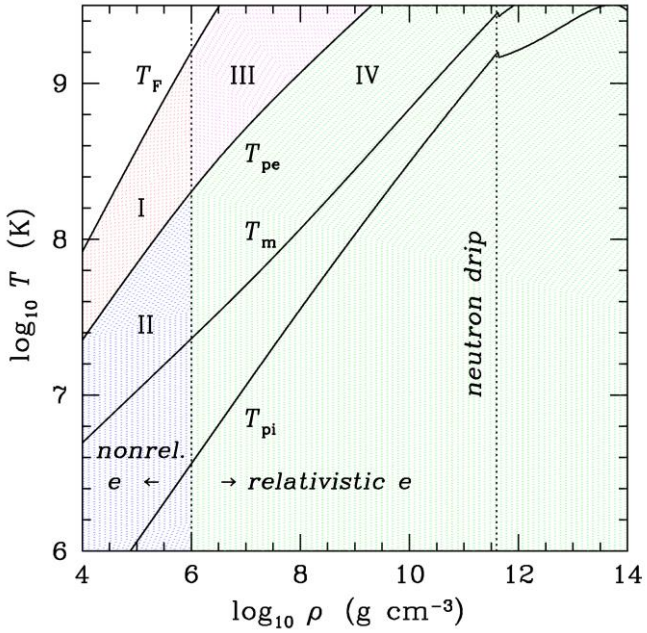


figure from Shternin & Yakovlev, PRD 74 043004 (2006)

non-FL behavior – is a relativistic effect $(v/c)^4$

NS core – regime 4

At high T (mergers?) can go to regime III: screening only logarithmically important

S. Stetina arXiv:1902.10745 (2109)

Neutron transport in NS cores

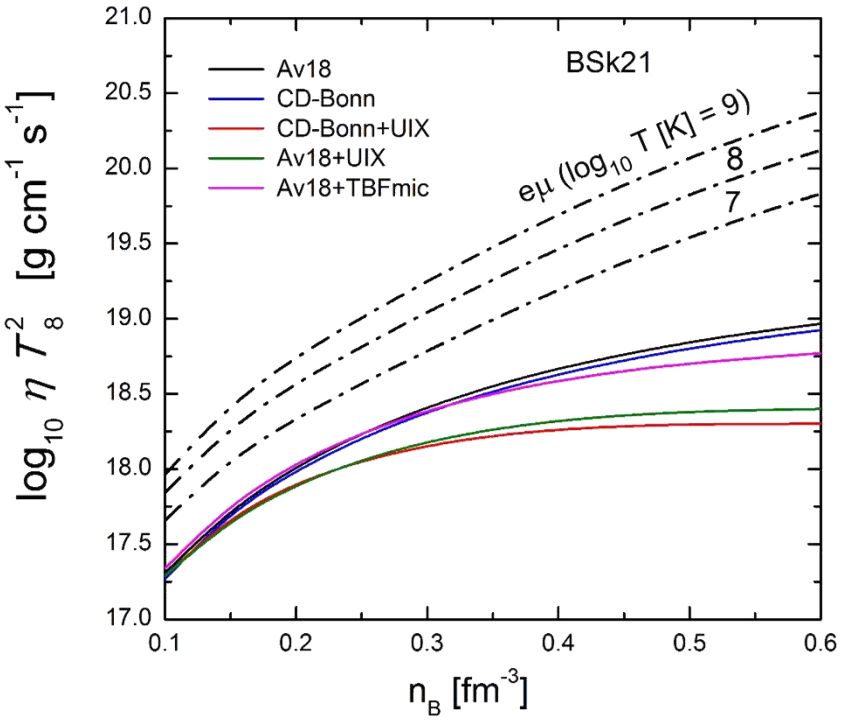
Shear viscosity and thermal conductivity

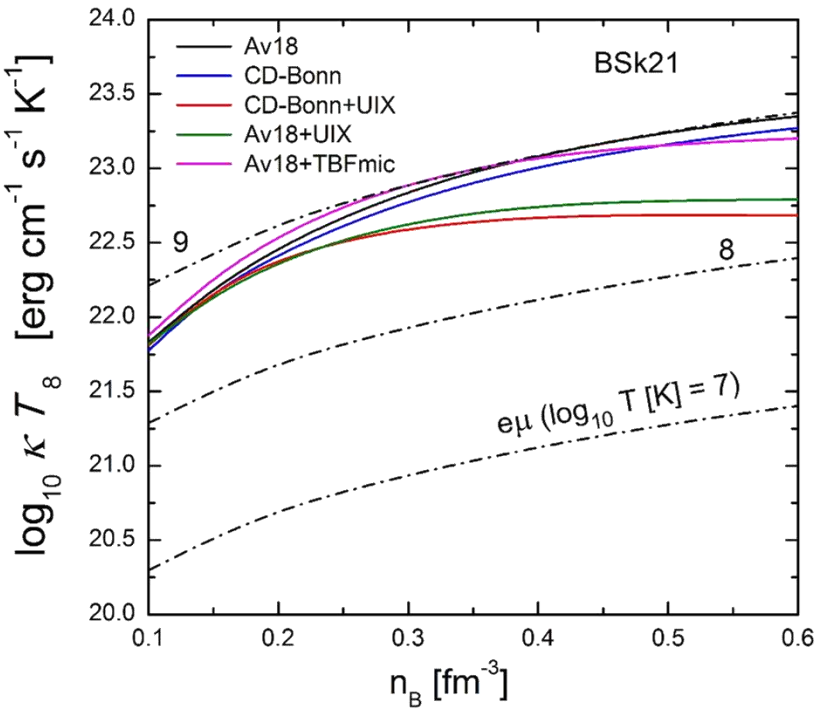
$$\eta_n \propto T^{-2}$$

$$\eta_{e\mu} \propto T^{-5/3}$$

$$\kappa_n \propto T^{-1}$$

$$\kappa_{e\mu} = \mathrm{const}(T)$$



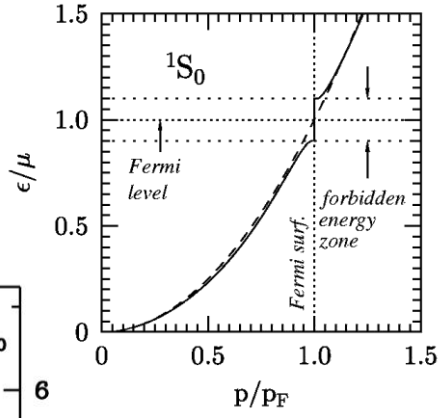


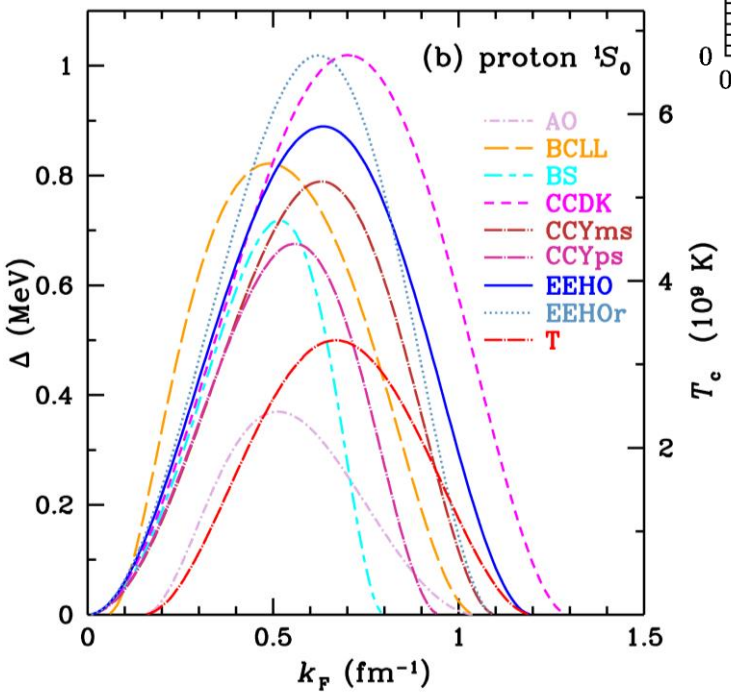
$$\eta_{e\mu} \gg \eta_n$$

$$\kappa_{e\mu} \ll \kappa_n$$

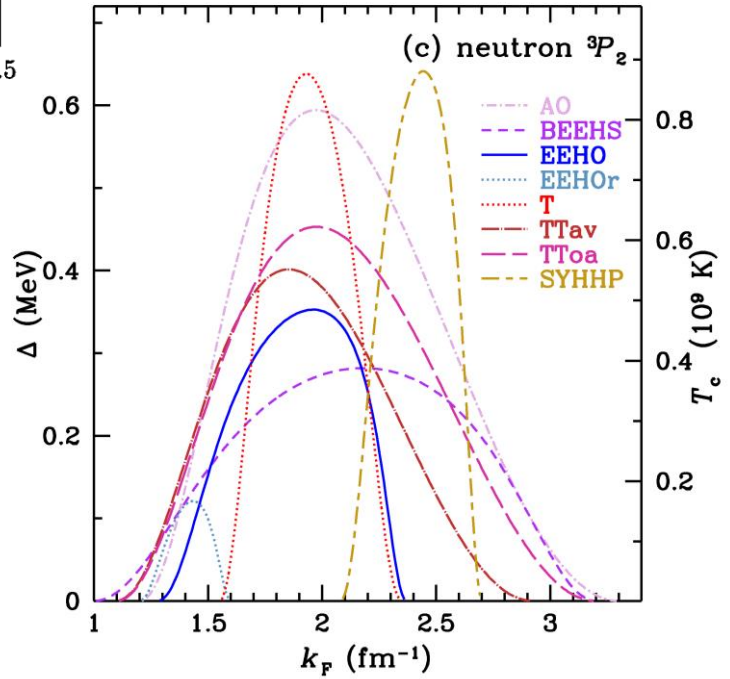
Pairing gaps in nucleon core of a NS

$^1S_0$ proton paring gaps





$^3P_2$ neutron paring gaps



$^1S_0$ neutron pairing is also expected in the inner crust

figures from W.C.G. Ho et al. PRC 91, 015806 (2015)

Neutron transport. Pairing

Two-fluid (SF) hydrodynamics

Normal component: transport by Bogoliubov excitations

$$\nu_n = \nu_{nn} + \nu_{np}$$

Collisions are suppressed $\nu \propto \exp(-\Delta/T)$

Only effect of gaps in spectrum is considered

Not elaborated up to now: accurate collision integral, including quasiparticle non-conservation; anisotropic transport in neutron superfluid

Collective modes (phonons, angulons)

Thermal conductivity

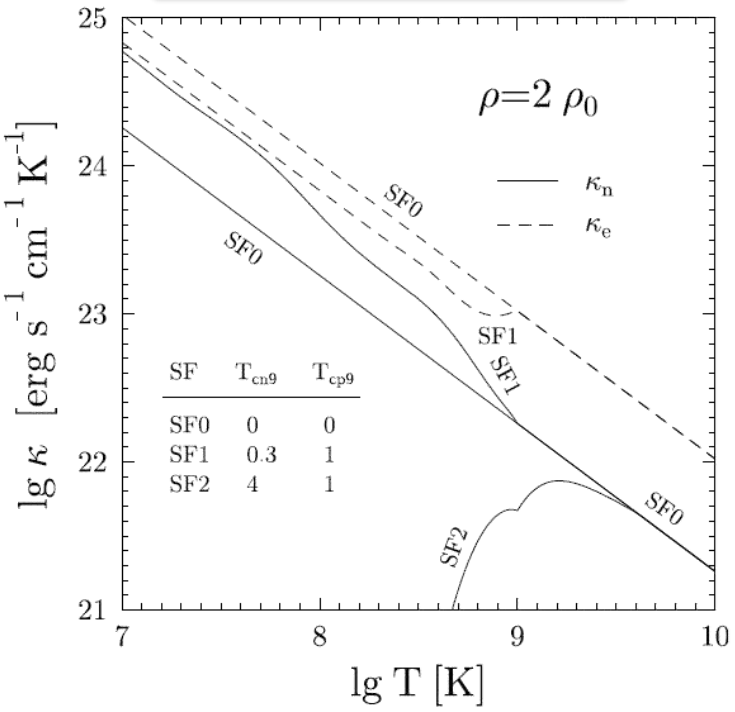


figure from Baiko et al., A&A 374, 151 (2001)

Manuel, Tolos 2011,2013; Kolomeitsev, Voskresensky 2015; Bedaque, Reddy 2014

Electron/muon transport in presence of proton pairing

Collisions with protons are suppressed at low T $\nu_{\ell p} \propto \exp(-\Delta/T)$

$$\nu_e = \nu_{ee} + \nu_{e\mu}$$

But lepton collisions are also affected since proton contribution to screening changes

Longitudinal screening not affected $\Pi_l^{\rm SF} \approx \Pi_l^{\rm N}$

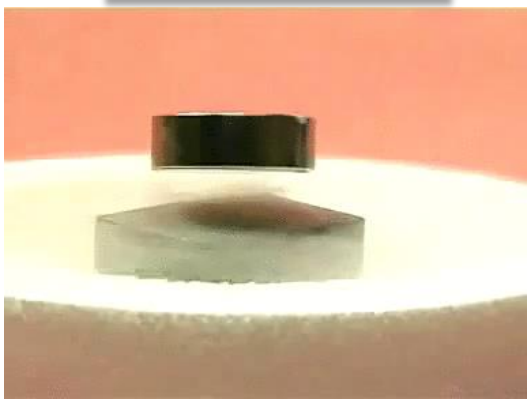
Transverse screening changes and becomes static

$$\Pi_t = \sum_i \Pi_{t,i}$$

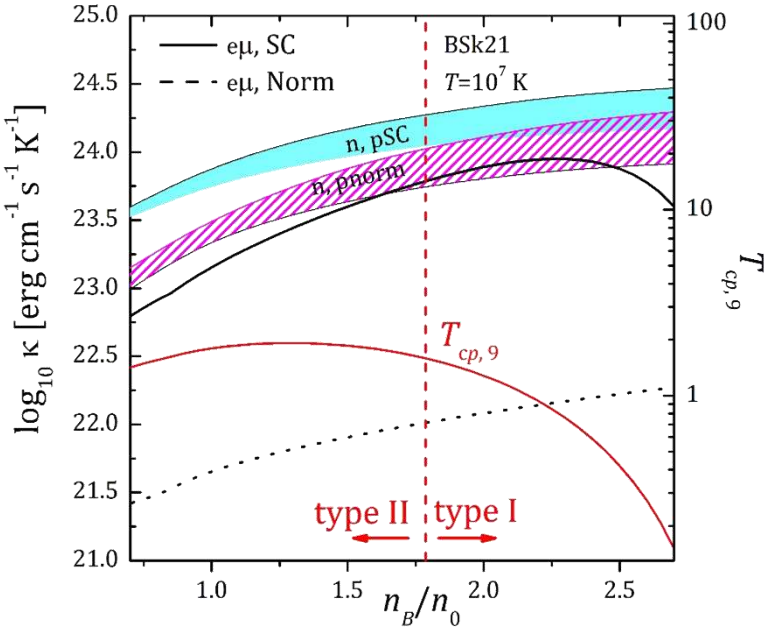
$$\Pi_{t,p}(\omega, q) = \Pi_{t,p}(0, q) \gg \Pi_{t,e/\mu}(\omega, q)$$

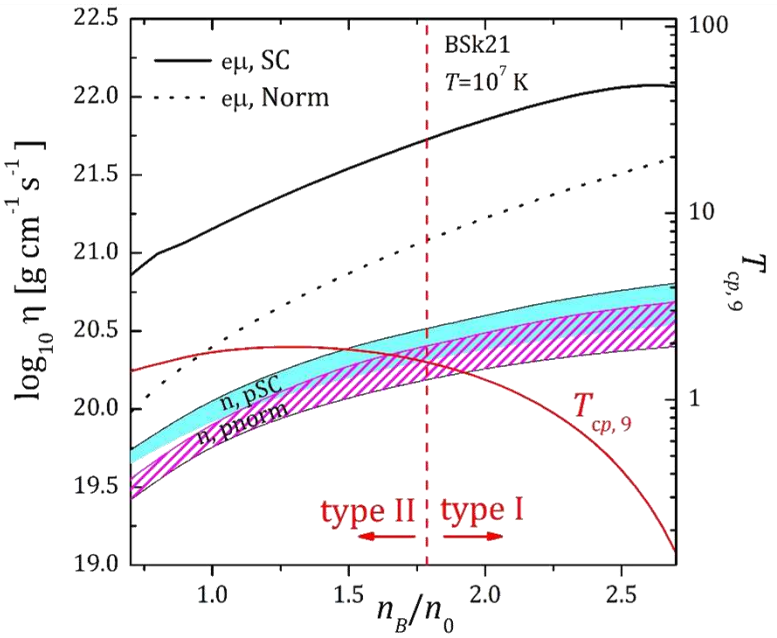
Temperature dependence restores $\nu_{ci} \propto T^2$

Meissner effect



Transport in NS cores. Paired protons





Relation between lepton and baryon transport coefficients persists

$$\kappa_{e\mu} \ll \kappa_n[nn]$$
$$\eta_{e\mu} \gg \eta_n[nn]$$

if SC of the type II

$$\frac{\pi\Delta}{v_{Fp}q_M} \equiv \varkappa > 1/\sqrt{2}$$

Do not depend on gap

$$\kappa_{e\mu}^{t,Lon} = \frac{5\,q_M^3}{18\pi^2\alpha_f^2 T} \qquad \eta_{e\mu}^{t,Lon} = \frac{6\,q_M}{5\alpha_f^2(k_B T)^2}\frac{n_e^2+n_\mu^2}{p_{Fe}^2+p_{F\mu}^2}$$

Shternin, PRD 98, 063015 (2018)

2SC quark matter. Effects of Pairing

unpaired (b) quarks and electrons

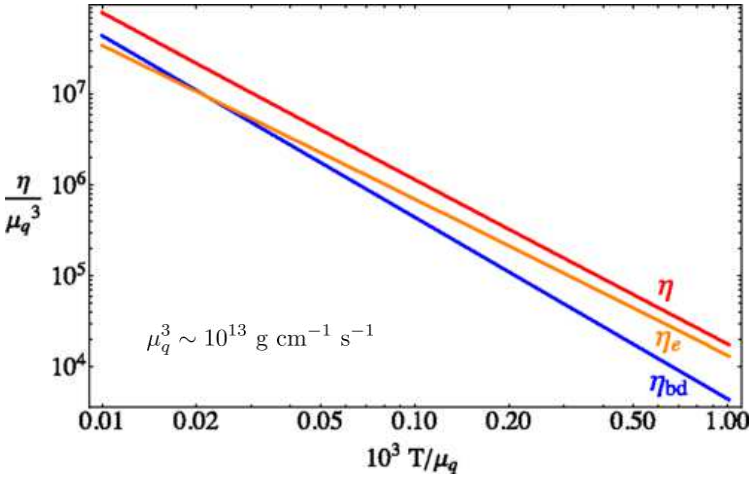
properties of g changes by red, green $\langle qq \rangle$

similar picture, but more cumbersome since g and γ mix

In CFL phase (fully gapped) superfluid phonons determine the transport. Caution: ballistic regime (large mean free paths, need to include GR…)

screening masses and charges

	T_8	Q	$\tilde{T}_8$	$\tilde{Q}$
	electric screening		magnetic screening	
screening mass	$3g^2$	$2e^2$	$g^2/3$	0
blue up	$-g/\sqrt{3}$	$2e/3$	$-g/\sqrt{3}$	e
blue down	$-g/\sqrt{3}$	$-e/3$	$-g/\sqrt{3}$	0
electron	0	$-e$	$-e^2/(g\sqrt{3})$	$-e$



M.G. Alford, H. Nishimura, A. Sedrakian, PRC 90, 055205 (2014)

Contents

Part I: Transport coefficients in NS core and crust

a) NS core
b) NS crust

Transport coefficients in NS crust-1

Structure of the crust

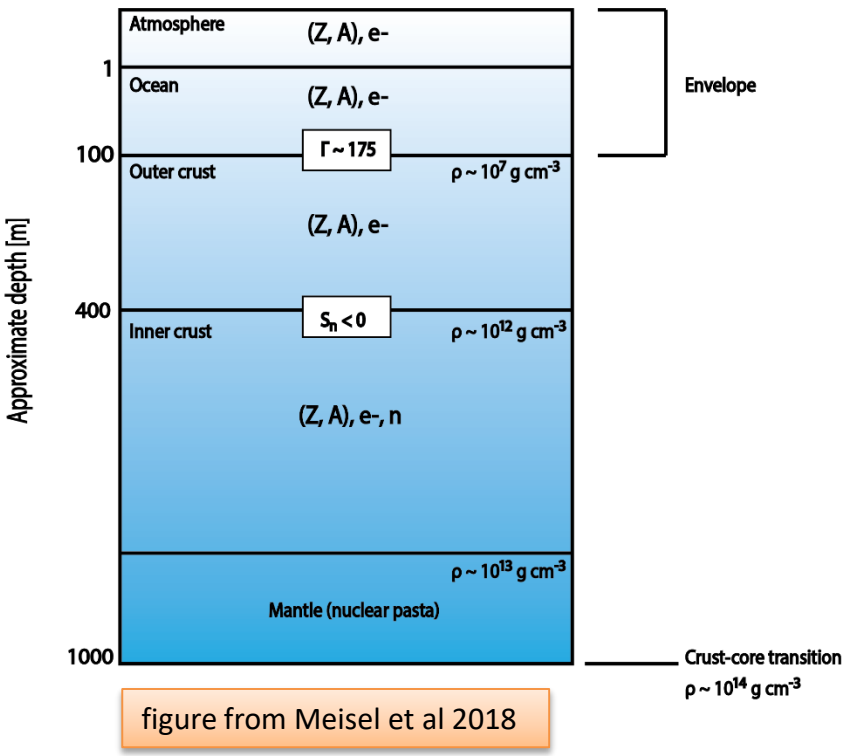


figure from Meisel et al 2018

Transport across melting point not fully understood (possible incipient long-range order in liquid)

Electron transport. Main contribution from electron-ion interactions (r.t.a. applicable at $T > 0.2\,T_{pi}$)

$$T_{\rm pi} \equiv \frac{\hbar\omega_{\rm pi}}{k_{\rm B}} = \frac{\hbar}{k_{\rm B}}\sqrt{\frac{4\pi Z^2 e^2 n_i}{A m_u}} \approx 1.9\times10^9\,{\rm K}\,\sqrt{\frac{Z}{A}}\left(\frac{\mu_e}{20\,{\rm MeV}}\right)^{3/2}$$

Strongly depends on the state of the system, described by the non-ideality parameter

$$\Gamma \approx 105\left(\frac{Z}{26}\right)^{5/3}\left(\frac{T}{10^8\ {\rm K}}\right)^{-1}\frac{\mu_e}{1\ {\rm MeV}}$$

Liquid ocean/amorphous solid:

$$\nu_{\rm ei} = \frac{4\alpha_f^2}{3\pi}\frac{\mu_{\rm e}}{\hbar}\frac{\langle Z^2\Lambda_{\rm ei}\rangle}{\langle Z\rangle} \qquad \Lambda_{ei} \sim 1$$

Perfect crystal: $\nu_{\rm ei} = \nu_{\rm e-ph} \approx 13\,\alpha_f\,\dfrac{k_{\rm B}T}{\hbar}$

Impurities (idealization)

$$\langle Z^2\Lambda_{\rm ei}\rangle \to Q_{\rm imp}\Lambda_{\rm imp}$$

$$Q_{\rm imp} \equiv \frac{1}{n_{\rm ion}}\sum_j n_j(Z_j - \langle Z\rangle)^2$$

Transport coefficients in NS crust-2

Ordered phase (crystalline): high conductivities (limited by impurities)

Disordered phase (liquid, glass): low conductivities

Transport across melting point not fully understood (possible incipient long-range order in liquid)

Order in multicomponent system (accreted crust)?

Can try to probe by observations (next slides)

Wiedemann-Franz rule (at $T > 0.2\ T_{pi}$)

$$\frac{\kappa}{\sigma} = \frac{\pi^2 k_B^2 T}{3e^2}$$

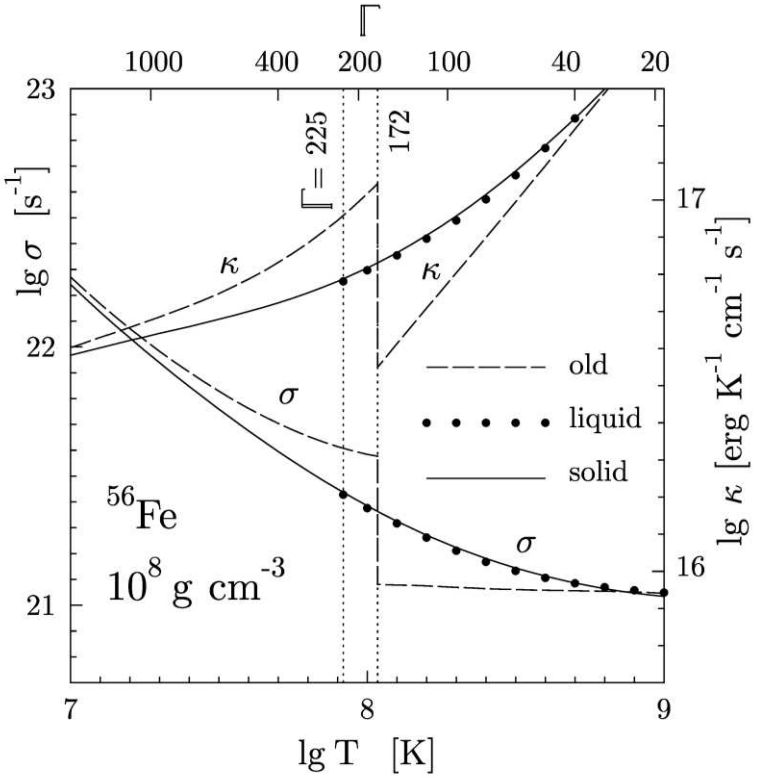
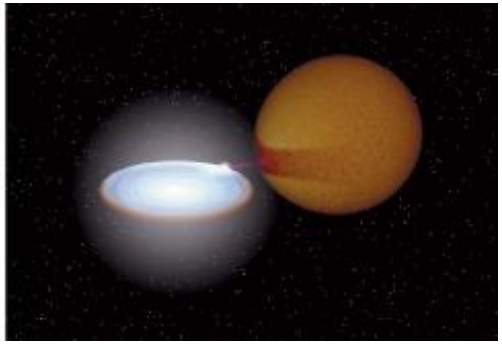


figure from Baiko et al., PRL 81, 5556 (1998)

Astro: Cooling of quasi-persistent LMXB-1



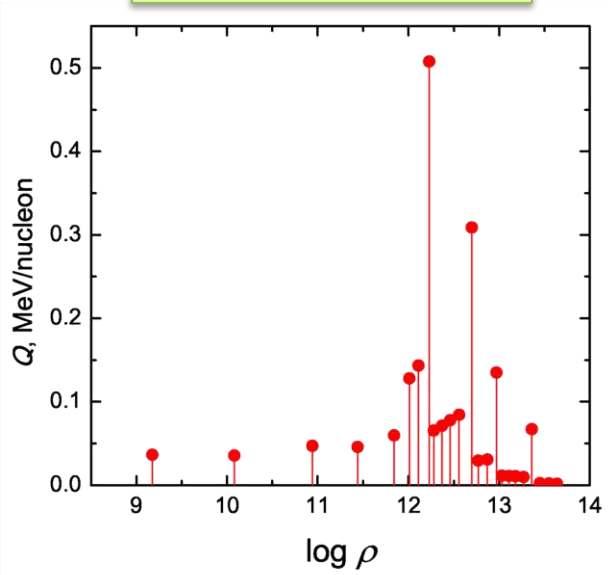
Most of the time in quiescence $L_q \sim 10^{32} - 10^{33}\ \mathrm{erg\ s^{-1}}$

With periodic outbursts $L_{\mathrm{ob}} \sim 10^{37} - 10^{38}\ \mathrm{erg\ s^{-1}}$

Deep crustal heating

Brown, Bildsten, Rutledge, 1998
Haensel, Zdunik, 1990, 2008

Heating sources



Heating due to nuclear transformations in accreted crust being compressed by fresh falling material

Mostly pycnonuclear reactions

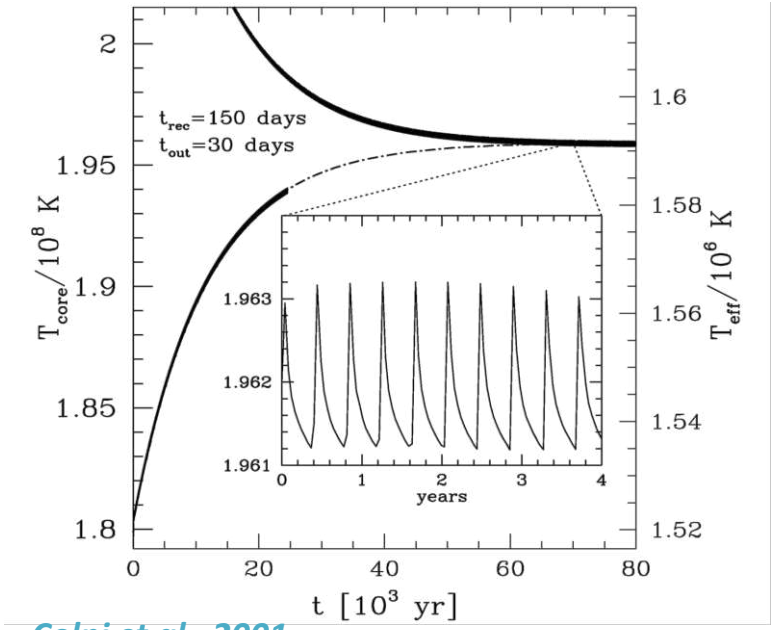
$Q_{\mathrm{tot}} \lesssim 2\ \mathrm{MeV/nucleon}$

Astro: Cooling of quasi-persistent LMXB-2

Two types of SXRTs

Type I (standard)

Short outbursts, many recurrences

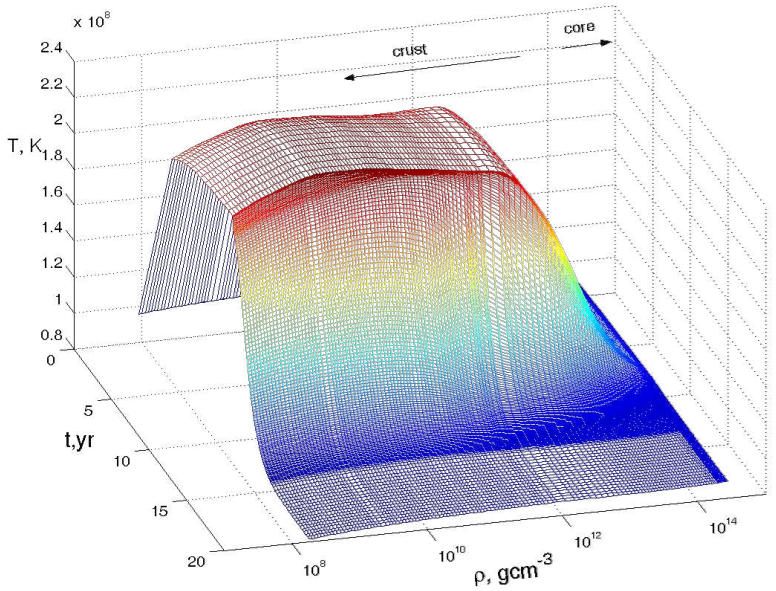


Colpi et al. 2001

All heat goes to core

Type II (quasi-persistent)

Long outbursts (years to decades)

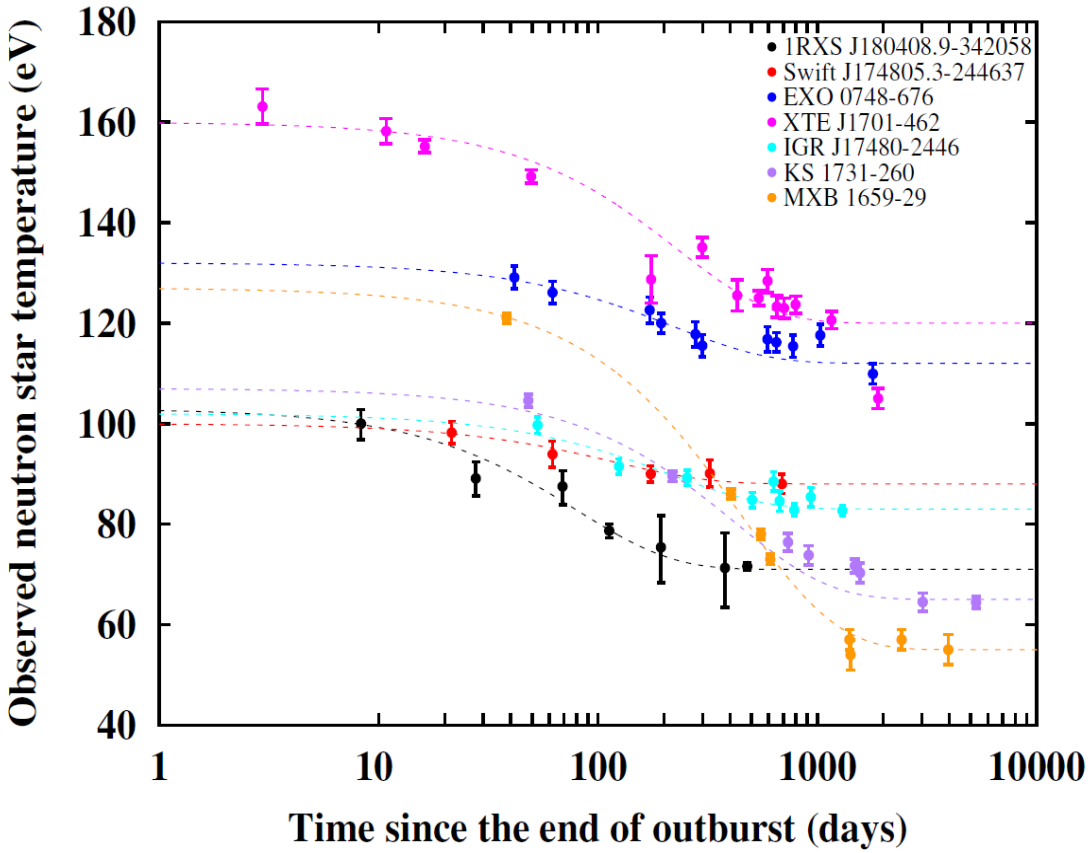


E.g. 13 yr outburst: overheated crust

Possible to observe crustal cooling

Astro: Cooling of quasi-persistent LMXB-3

Crustal cooling in type-II transients is actually observed



Cooling timescale

$$\tau = \frac{1+z}{4}\left[\int_0^y \left(\frac{c_P}{\rho\kappa}\right)^{1/2} \mathrm{d}y'\right]^2,$$

Probes the structure and transport properties of the crust

figure from Wijnands, Degenaar, & Page, J Astrophys. Astron. 38, 49 (2017)

Astro: Cooling of KS 1731-260

The first source with the detailed crustal cooling curve
Deep crustal heating model explains successfully

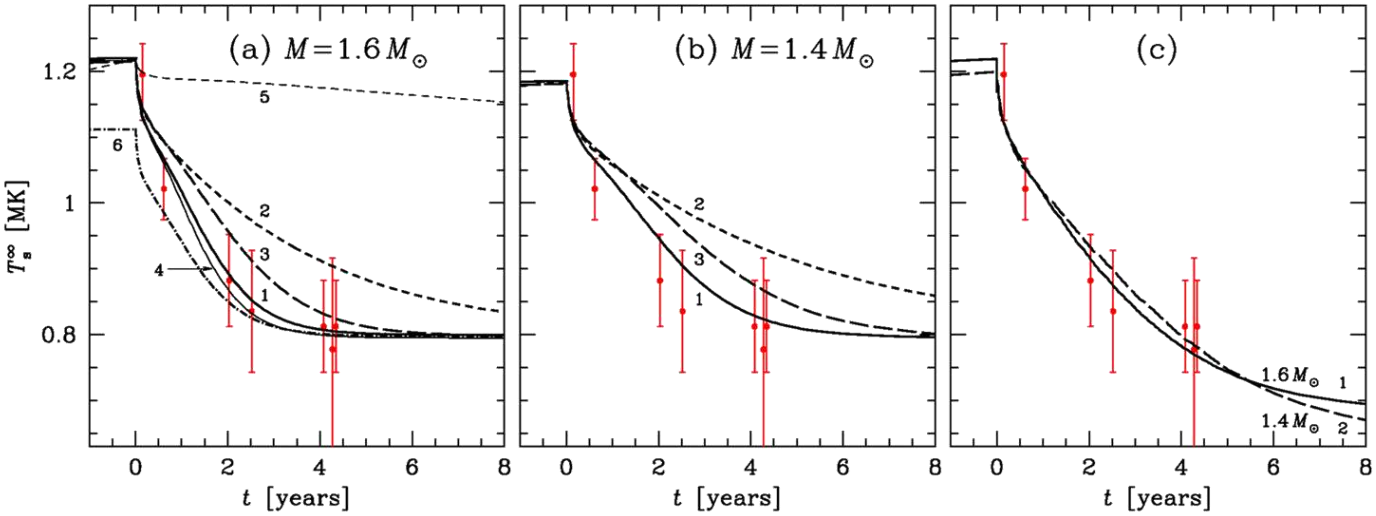


figure from Shternin et al (2007)

- High conductivity hence ordered structure (curve 5 – for amorphous crust)

Today status:

- unknown additional shallow heating source ~ 1 MeV/nucleon
- how to obtain order in multicomponent case (next slide)?

Brown, Cumming (2009); Wijnands et al. (2017)

Astro: Ashes of surface burning

Ash production on the surface leads to very diverse composition. How to produce perfect ordering?

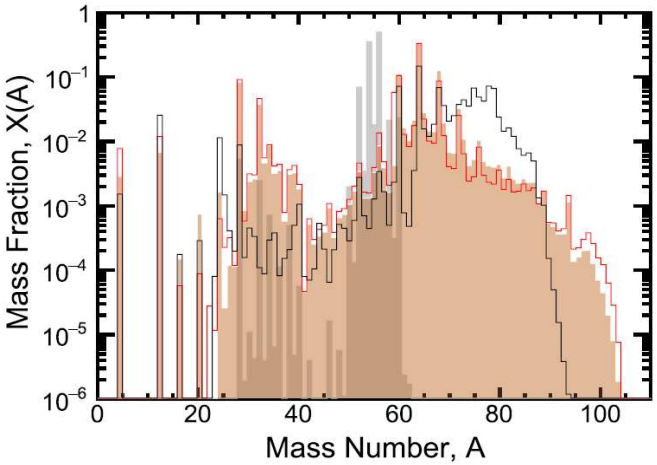
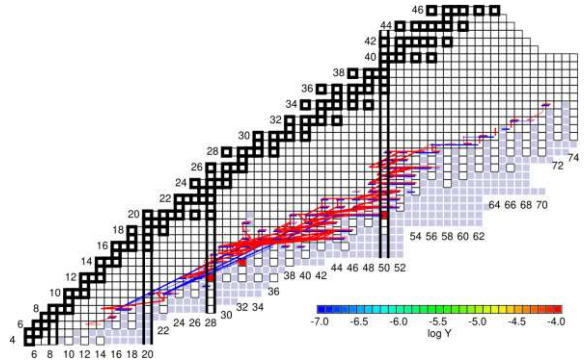
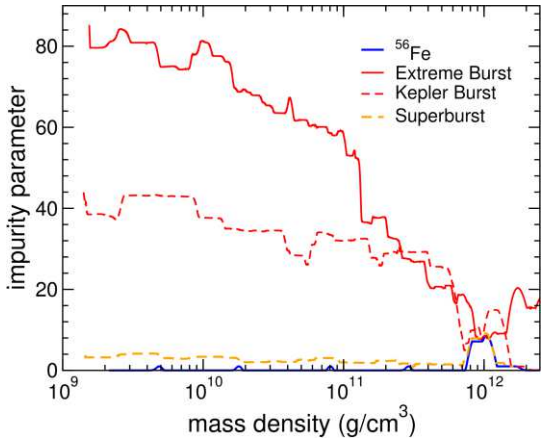


Figure 4. Ash abundances predicted for stable surface burning at near-Eddington acretion rate (black-lined unfilled histogram), superbursts (gray-filled histogram), and Type-I x-ray bursts for a nominal reaction rate library (red-filled translucent histogram) and, to highlight the impact of nuclear physics uncertainties, for the ^{59}Cu(p, γ) rate reduced by a factor of 100 (red-lined unfilled histogram). Calculation details are described in [26]. General ash properties are listed in table 1.

figure from Meisel et al 2018

Reaction network calculations





figures from Lau et al 2018

Complications: Transport coefficients in mantle

Pasta phases at a crust-core interface

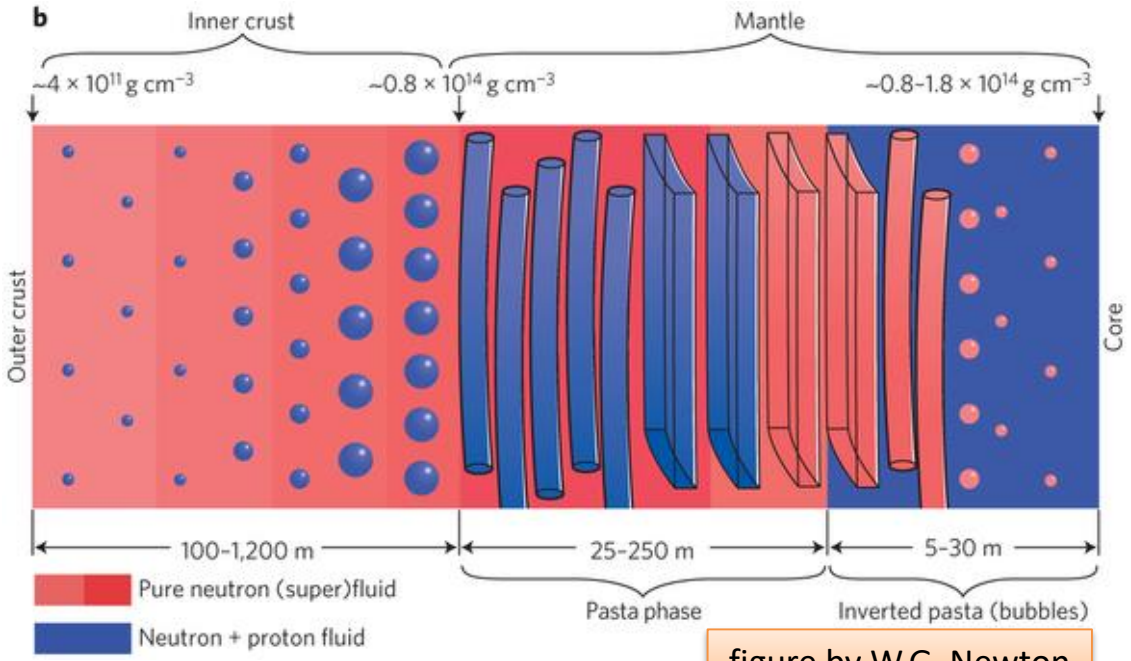


figure by W.G. Newton

Highly resistive/thermal insulating layer in pasta was proposed (emulated by large Q_{imp})
Two examples:

Large Q_{imp} is not physical, actually
(clearly not the case of `a few impurities here and there')

(κ): $Q_{imp} \sim 40$ by Horowitz et al. 2015 for late-time cooling stage of LMXB MXB 1659—29
(σ): $Q_{imp} \sim 100$ by Pons et al. 2013 for magnetic field decay and long-periodic pulsars

Complications: Transport coefficients in pasta

Coulomb logarithm

$$\Lambda_{ei}^{\kappa,\sigma} = \int_0^{2k_{Fe}} \frac{dk}{k} |k^2 U(k)|^2 \left[1 - \frac{k^2}{4m_e^{*2}}\right] S(k)$$

Ion correlations: structure factor

$$S(\boldsymbol{k}) = \frac{1}{N_\mathrm{i}} \int d^3\boldsymbol{x}\, d^3\boldsymbol{x}'\, e^{i\boldsymbol{k}\cdot(\boldsymbol{x}-\boldsymbol{x}')} \left\langle \delta\hat{n}^\dagger(\boldsymbol{x},t)\delta\hat{n}(\boldsymbol{x}',t)\right\rangle_{\mathrm{eq}}$$

S(k) calculated directly form large molecular dynamics simulations

Nandi & Schramm Apj 852, 135 (2018); Schneider et al. PRC 98, 055801 (2018)

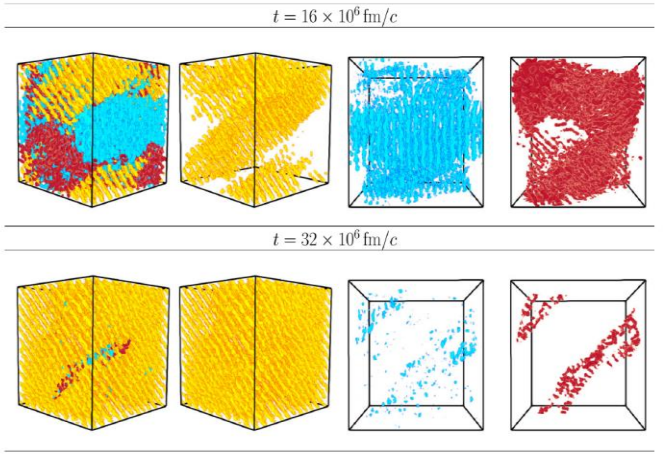


FIG. 10. Similar to Fig. 7 but for the 1 638 400 nucleon system at times $t = 16$ and 32×10^6 fm/c.

Not much difference in averaged <S(k)>

However – anisotropic case: different relaxation times along different pasta symmetry axes.
Complication: domains

how to include pasta order (Bragg structure)?

$$I[f] = -\frac{\partial f^{(0)}}{\partial \varepsilon} \left[\nu_a(\varepsilon) w_z \vartheta_z + \nu_p(\varepsilon) \boldsymbol{w}_p \cdot \boldsymbol{\vartheta}_p\right]$$

Open problem

D.G. Yakovlev, MNRAS 453, 581 (2015)

Magnetic field effects in crust /skip/

Magnetic field makes transport anisotropic
transport coefficients now are tensor quantities
quantization (electron motion in the crust)

$$\kappa,\ \sigma \rightarrow \hat{\kappa},\ \hat{\sigma}$$

$$\hat{\tau} = \begin{pmatrix} \tau_\perp & \tau_\Lambda & 0 \\ -\tau_\Lambda & \tau_\perp & 0 \\ 0 & 0 & \tau_\parallel \end{pmatrix}$$

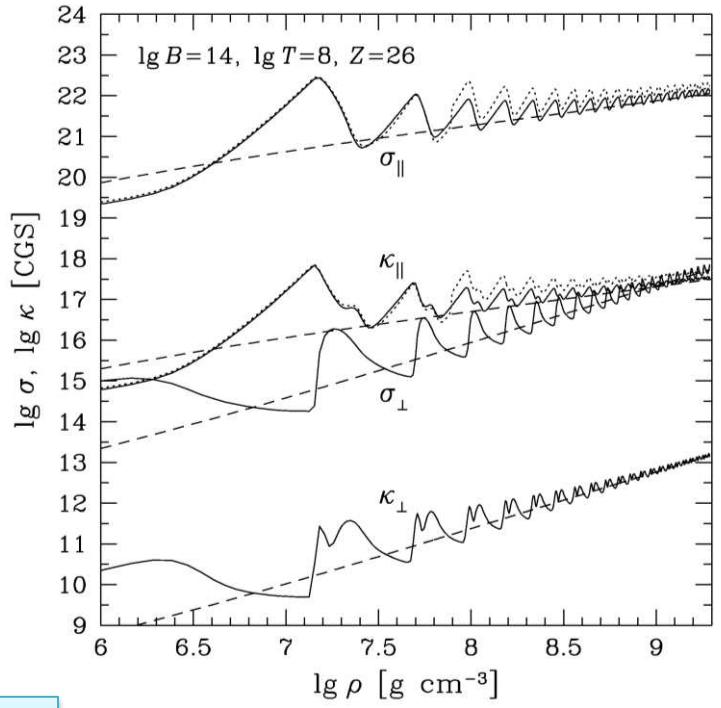
$$\tau_\parallel = \tau$$

In non-quantizing field

$$\tau_\perp = \frac{\tau}{1+(\omega_g\tau)^2} \qquad \tau_\Lambda = \frac{\omega_g\tau^2}{1+(\omega_g\tau)^2}$$

$$\omega_g\tau = 1760\frac{B_{12}}{\sqrt{1+x_r^2}}\frac{\tau}{10^{-16}\ \mathrm{s}}$$

A.Y. Potekhin, A&A 351, 787 (1999)



Five shear viscosity coefficients (spatial rank 2)

in magnetized pasta: 2 anisotropy sources (hence, e.g., two Hall components)

Electrical conductivity in magnetized core /skip/

Diffusion in multicomponent magnetized mixture

$$-\frac{\mu_i n_i}{c^2}\dot{\boldsymbol{v}} + \boldsymbol{F}_i + \frac{q_i n_i}{c}\boldsymbol{\vartheta}_i \times \boldsymbol{B} = \sum_j J_{ij}(\boldsymbol{\vartheta}_i - \boldsymbol{\vartheta}_j)$$

J_{ij} – transport coefficients (momentum relaxation rates)

In the co-moving frame

$$\boldsymbol{F}_i = q_i n_i \boldsymbol{E}' \equiv q_i n_i \left(\boldsymbol{E} + \frac{1}{c}\boldsymbol{v} \times \boldsymbol{B}\right)$$

Generalized Ohm law $\boldsymbol{E}' = \hat{\mathcal{R}}\boldsymbol{j}$

Example: resistivity in npe matter

$$\mathcal{R}_\parallel = [\sigma(B=0)]^{-1}\,, \qquad \mathcal{R}_\perp = \mathcal{R}_\parallel + \frac{X_n^2}{J_{pn}c^2}B^2\,, \qquad \mathcal{R}_\Lambda = \frac{1-2X_e}{n_e e c}B$$

Transverse resistivity increases with B due to np friction (i.e. ambipolar diffusion)

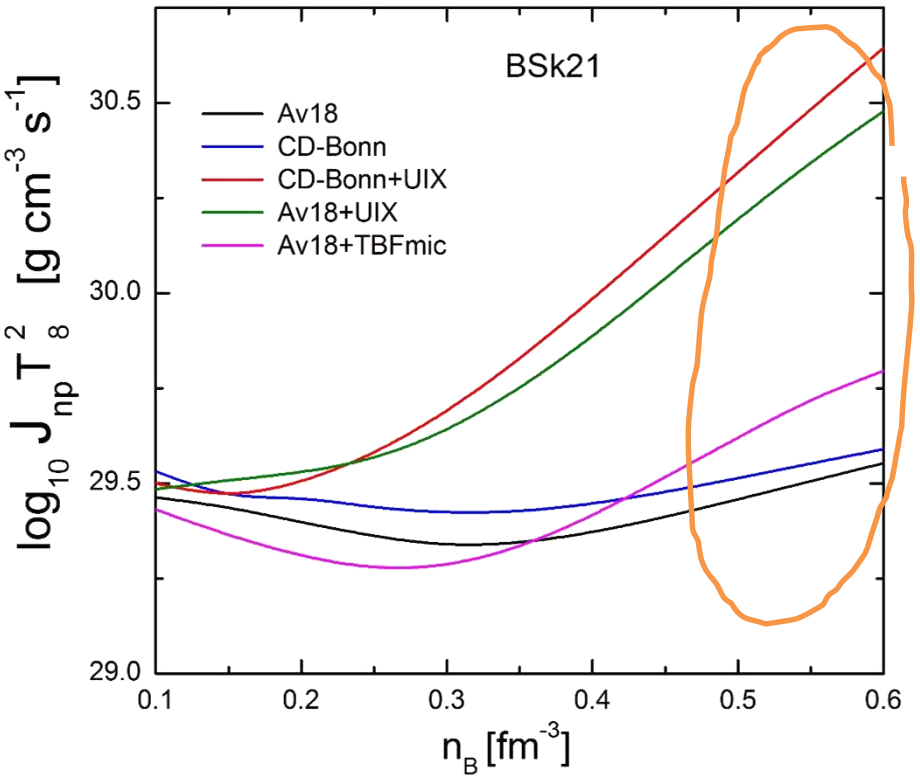
Haensel et al. (1990)

Dissipation (entropy generation)

$$T\varsigma|_{\rm coll} = \frac{1}{2}\sum_{ij} J_{ij}(\boldsymbol{\vartheta}_i - \boldsymbol{\vartheta}_j)^2 = \boldsymbol{j}\boldsymbol{E}' = j_\parallel^2\mathcal{R}_\parallel + j_\perp^2\mathcal{R}_\perp$$

Neutron-proton friction in BHF model /skip/

Momentum relaxation rates calculated from the kinetic theory as above



Order of magnitude uncertainty in B-field decay timescale at high density

$$t_B^{\rm amb} \sim \frac{J_{\rm np} R^2}{B^2}$$

Part II: Neutrino-generating reactions

Main ingredient in NS cooling studies

$$C\frac{\mathrm{d}\widetilde{T}}{\mathrm{d}t} = -L_\nu^\infty - L_\gamma^\infty + L_{\rm heat}$$

See next talks

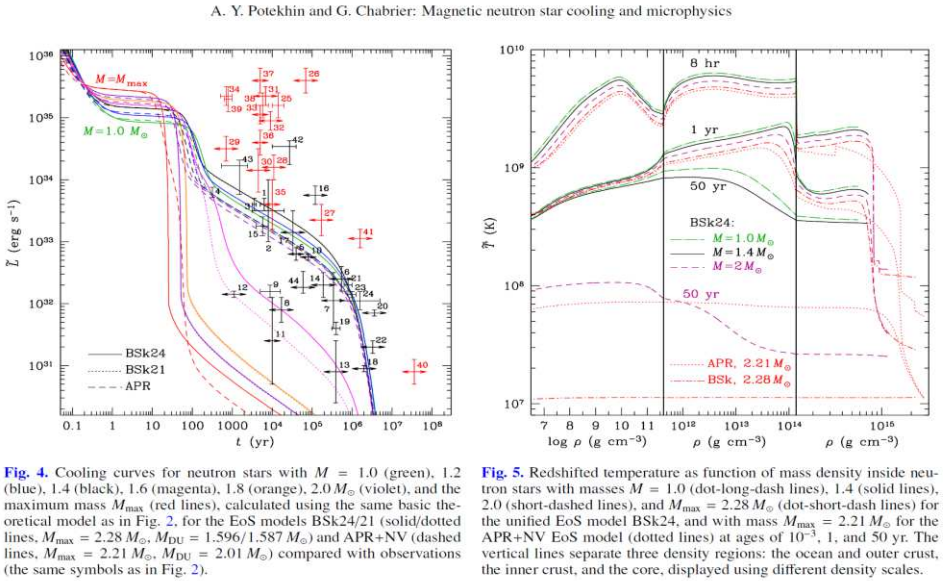


Fig. 4. Cooling curves for neutron stars with M = 1.0 (green), 1.2 (blue), 1.4 (black), 1.6 (magenta), 1.8 (orange), 2.0 $M_\odot$ (violet), and the maximum mass $M_{\rm max}$ (red lines), calculated using the same basic theoretical model as in Fig. 2, for the EoS models BSk24/21 (solid/dotted lines, $M_{\rm max}$ = 2.28 $M_\odot$, $M_{\rm DU}$ = 1.596/1.587 $M_\odot$) and APR+NV (dashed lines, $M_{\rm max}$ = 2.21 $M_\odot$, $M_{\rm DU}$ = 2.01 $M_\odot$) compared with observations (the same symbols as in Fig. 2).

Fig. 5. Redshifted temperature as function of mass density inside neutron stars with masses M = 1.0 (dot-long-dash lines), 1.4 (solid lines), 2.0 (short-dashed lines), and $M_{\rm max}$ = 2.28 $M_\odot$ (dot-short-dash lines) for the unified EoS model BSk24, and with mass $M_{\rm max}$ = 2.21 $M_\odot$ for the APR+NV EoS model (dotted lines) at ages of 10^{-3}, 1, and 50 yr. The vertical lines separate three density regions: the ocean and outer crust, the inner crust, and the core, displayed using different density scales.

figure from Potekhin, Chabrier 2018

Neutrino emission in the crust /skip/

Main mechanisms

Plasmon decay $\gamma \rightarrow \nu + \bar{\nu}$

Bremsstrahlung $e + Z \rightarrow e + Z + \nu + \bar{\nu}$

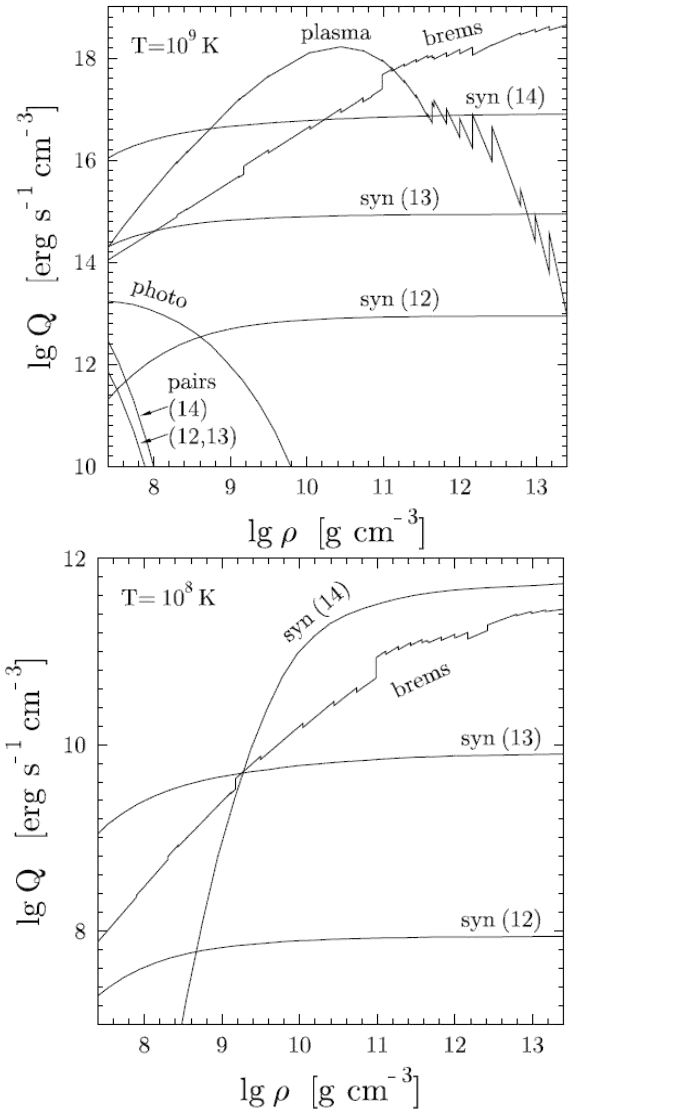
$n + n \rightarrow n + n + \nu + \bar{\nu}$

Pair annihilation $e + e^{+} \rightarrow \nu + \bar{\nu}$

Photo-neutrino $e + \gamma \rightarrow e + \nu + \bar{\nu}$

Synchrotron $e + \boldsymbol{B} \rightarrow e + \boldsymbol{B} + \nu + \bar{\nu}$

Important for early cooling and non-equilibrium processes in the crust (e.g., superbursts)



figures from Yakovlev et al., Phys. Rep. 354, 1 (2001)

Weak reactions in NS cores

Neutrino reactions are mainly the source for cooling (neutrino escapes freely, cf. SNe)
Degenerate matter : each fermion adds $T/\mu \Rightarrow$ classified by N_f

Charged weak current reactions: Direct Urca (DUrca)

$$\begin{aligned} \mathcal{B}_1 &\rightarrow \mathcal{B}_2 + \ell + \bar{\nu}_\ell, \\ \mathcal{B}_2 + \ell &\rightarrow \mathcal{B}_1 + \nu_\ell \end{aligned} \qquad \begin{aligned} Q_\nu &\sim 10^{27} T_9^6 \ \frac{\mathrm{erg}}{\mathrm{s\,cm^3}} \\ L_\nu &\sim 10^{46} T_9^6 \ \mathrm{erg/s} \end{aligned}$$

! threshold process ($p_{F1} < p_{F2} + p_{F\ell}$). In npe matter $x_p > 11\%$

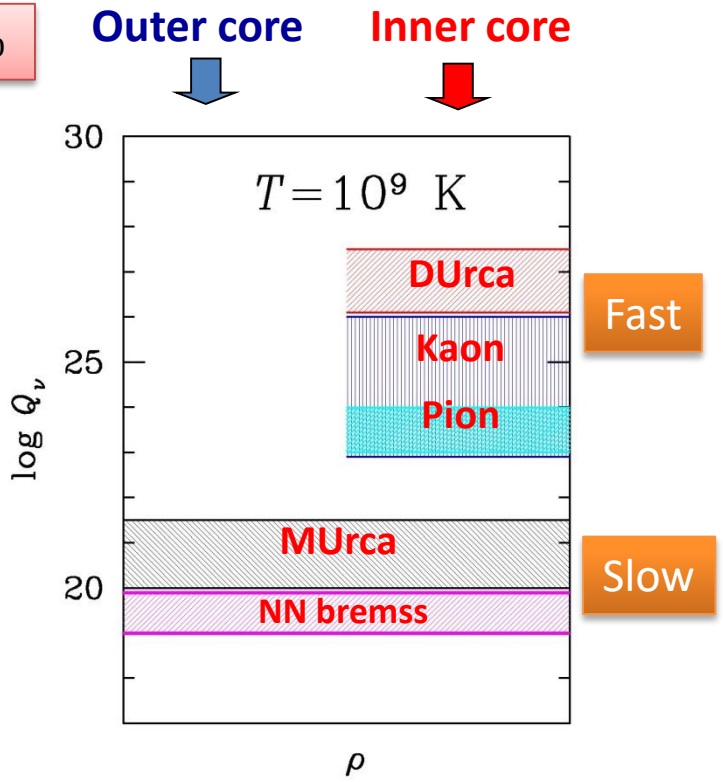
2nd order: neutral weak current reactions: bremsstrahlung

$$\mathcal{B}_1 + \mathcal{C} \rightarrow \mathcal{B}_1 + \mathcal{C} + \bar{\nu}_\ell + \nu_\ell$$

2nd order: charged weak current: modified Urca (mUrca)
no threshold => main process

$$\begin{aligned} \mathcal{B}_1 + \mathcal{C} &\rightarrow \mathcal{B}_2 + \mathcal{C} + \ell + \bar{\nu}_\ell \\ \mathcal{B}_2 + \mathcal{C} + \ell &\rightarrow \mathcal{B}_1 + \mathcal{C} + \nu_\ell \end{aligned} \qquad \begin{aligned} Q_\nu &\sim 10^{20} - 10^{21} T_9^8 \ \frac{\mathrm{erg}}{\mathrm{s\,cm^3}} \\ L_\nu &\sim 10^{39} T_9^8 \ \mathrm{erg/s} \end{aligned}$$

quark cores: direct Urca;
hyperon core: direct Urca, modified Urca
exotica: pion or kaon condensation



Weak reactions in NS cores

Consider flavor-changing reactions, e.g.

$$\begin{aligned} \mathcal{B}_1 &\rightarrow \mathcal{B}_2 + \ell + \bar{\nu}_\ell, \\ \mathcal{B}_2 + \ell &\rightarrow \mathcal{B}_1 + \nu_\ell \end{aligned}$$

In equilibrium

$$\sum_{\text{rhs}} \mu_i = \sum_{\text{lhs}} \mu_i$$

Forward and backward reaction rates are equal

$$\Gamma_{\leftarrow} = \Gamma_{\rightarrow}$$

Non-equilibrium situation (oscillations, currents induced by magnetic field, rotation)

$$\delta\mu = \sum_{\text{rhs}} \mu_i - \sum_{\text{lhs}} \mu_i$$

Affinity (chemical potential imbalance)

Chemical equilibration (linear regime)

$$\Delta\Gamma = \Gamma_{\leftarrow} - \Gamma_{\rightarrow} = \lambda\delta\mu \qquad \lambda > 0$$

Entropy generation

$$T\varsigma = \Delta\Gamma\delta\mu - Q_\nu = \lambda\delta\mu^2 - Q_\nu$$

In non-equilibrium case, reactions can either heat or cool the star

Electroweak bremsstrahlung in NS cores

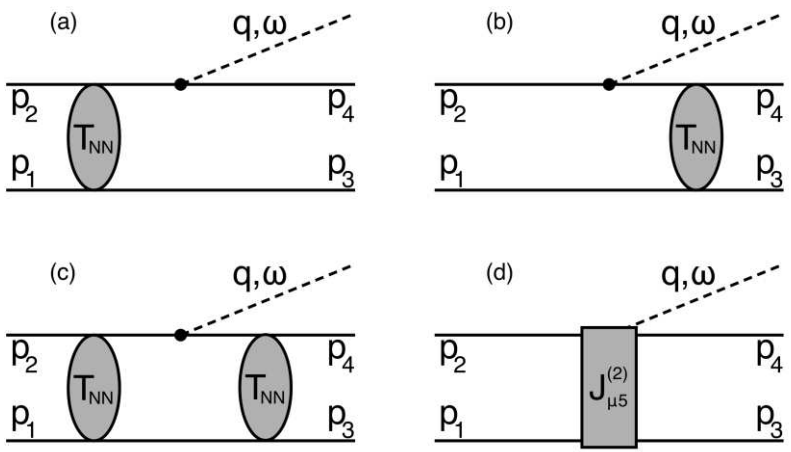
Let the Direct Urca is forbidden
Next-order reactions: $NN\nu\tilde{\nu}, NN\ell\nu$

In quasi-particle approximation, reaction rates and emissivities can be computed from Fermi's Golden Rule

$$\begin{pmatrix} \Gamma \\ Q_\nu \end{pmatrix} = \int \prod_{j=i,f} \frac{d^3\boldsymbol{p}_j}{(2\pi)^3} \mathcal{F}_{fi} (2\pi)^4 \delta^{(4)} (P_f - P_i) \begin{pmatrix} 1 \\ \omega_\nu \end{pmatrix} s \, |M_{fi}|^2$$

Likewise the transport coefficients, need to know effective masses and matrix elements with in-medium corrections

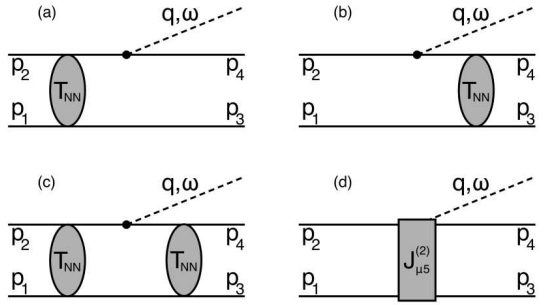
In contrast to transport coefficients calculations
1) the amplitudes are (half) on-shell
2) additional processes are involved



C. Hanhart et al., PLB 499, 9 (2001)

Electroweak bremsstrahlung in NS cores

Benchmark in NS studies: Friman & Maxwell 1979 model:
OPE exchange + medium effects via Landau parameters



$$Q_\nu^{nn} = 7.5\times10^{11}\left(\frac{m_n^*}{m_N}\right)^4\left(\frac{n_n}{n_0}\right)^{1/3}\left(\frac{T}{10^8\,\mathrm{K}}\right)^8 \alpha_{nn}^{\mathrm{ex}}\beta_{nn}\mathcal{N}_\nu \ \mathrm{erg\ cm^{-3}\ s^{-1}}$$

$$Q_\nu^{\mathrm{MU}} = 8.1\times10^{13}\left(\frac{m_n^*}{m_n}\right)^3\left(\frac{m_p^*}{m_p}\right)^4\left(\frac{p_{F\ell}c}{\mu_\ell}\right)\left(\frac{n_p}{n_0}\right)^{1/3}\left(\frac{T}{10^8\ K}\right)^8 \alpha_{\mathrm{MU}}^{n\ell}\ \mathrm{erg\,cm^{-3}\,s^{-1}}$$

$$\alpha_{\mathrm{MU}}^{n\ell}\approx 1 \qquad \alpha_{nn}^{\mathrm{ex}}\approx 0.8$$

Going beyond OPE approximation: soft bremsstrahlung theorem (diagram (b))

$$M_{fi}\propto\langle f|\hat{\mathbf{\Gamma}}^{Z/W}\mathcal{G}_N(\boldsymbol{p}_2-\boldsymbol{q};\varepsilon_2-\omega)T_{NN}|i\rangle$$

C. Hanhart et al., PLB 499, 9 (2001); Timmermans et al., PRC 65, 064007 (2002), van Dalen et al., PRC 67, 065807 (2003)

In soft limit, $\mathcal{G}_N(\boldsymbol{p}_2-\boldsymbol{q};\varepsilon_2-\omega)\approx\omega^{-1}$

For nn bremsstrahlung, $\omega\sim k_BT$

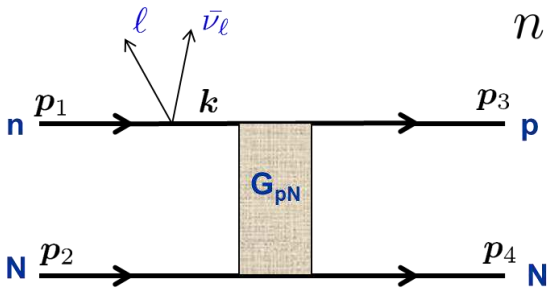
$$\boldsymbol{M}^{ax}=\frac{g_A}{\omega}[T_{NN},\boldsymbol{S}]_{fi}$$

Result

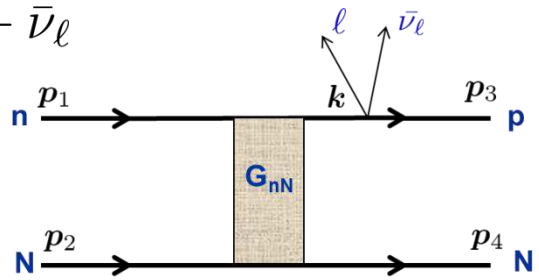
$$\hat{V}_{\mathrm{OPE}}\to\hat{T} \quad\Rightarrow\quad \alpha_{nn}^{\mathrm{ex}}\to 0.2$$
$$\hat{T}\to\hat{G}_{\mathrm{BHF}} \quad\Rightarrow\quad \alpha_{nn}^{\mathrm{ex}}\to 0.26$$

For modified Urca emitted energy is not small ($\omega\sim\mu_\ell$), SBT ?

Modified Urca in beta-stable matter



$$n + N \to p + N + \ell + \bar{\nu}_\ell$$



$$+Exch.$$

$$M_{fi} : \mathcal{G}(\boldsymbol{k}) \cdot \langle \boldsymbol{p}_3 \boldsymbol{p}_4 | \hat{G}_{\rm pN} | \boldsymbol{k} \boldsymbol{p}_1 \rangle$$

Beta-stability condition $E_n(p_1) - E_\ell(p_\ell) = E_{Fn} - E_{F\ell} = E_{Fp}$

Proton propagator

$$\mathcal{G}_p = \frac{i}{E_n(p_1) - E_\ell(p_\ell) - E_p(k) - E_\nu}$$

$$\mathcal{G}_p = \frac{i}{\mu_p - E_p(k) - E_\nu}$$

$$k = |\boldsymbol{p}_1 - \boldsymbol{p}_\ell| \geqslant p_{Fn} - p_{F\ell} > p_{Fp}$$

softening at $k \to p_{Fp}$

Backward scattering dominates. Two consequences:

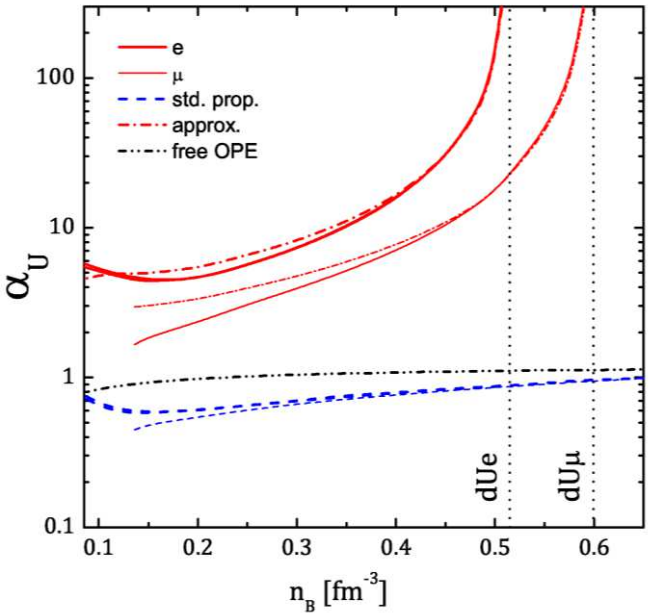
1) strong enhancement with density approaching the DUrca threshold
2) Close to on-shell amplitude needed: SBT analogue

Enhanced MUrca cooling

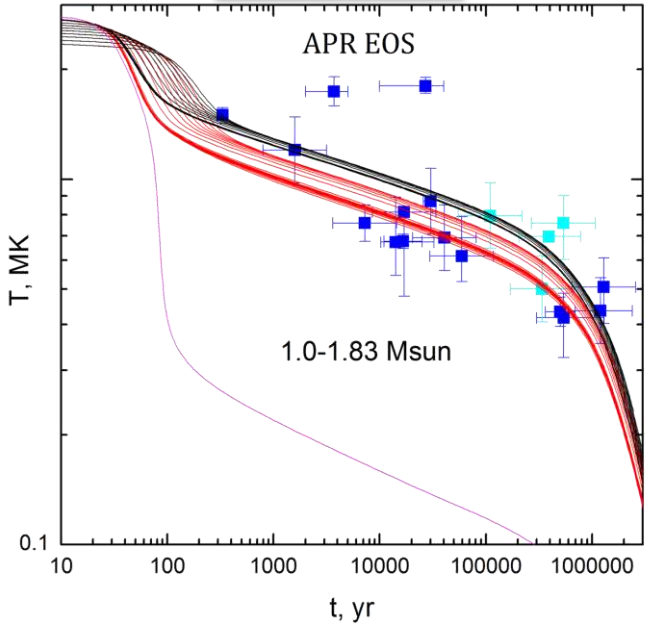
MUrca, neutron branch: $n + n \to p + n + \ell + \bar{\nu}_\ell, \quad p + n + \ell \to n + n + \nu_\ell$

$$Q_\nu^{\rm MU} = 8.1{\times}10^{13} \left(\frac{m_n^*}{m_n}\right)^3 \left(\frac{m_p^*}{m_p}\right)^4 \left(\frac{p_{F\ell} c}{\mu_\ell}\right) \left(\frac{n_p}{n_0}\right)^{1/3} \left(\frac{T}{10^8\ K}\right)^8 \alpha_{\rm MU}^{n\ell}\ {\rm erg\ cm^{-3}\ s^{-1}}$$

Dimensionless emissivity



NS cooling



G-matrix alone – small modification (dashed)

Mean field in propagator leads to enhancement and pronounced density dependence (solid)

P.S. Shternin, M. Baldo, P. Haensel, PLB 786, 28 (2018)

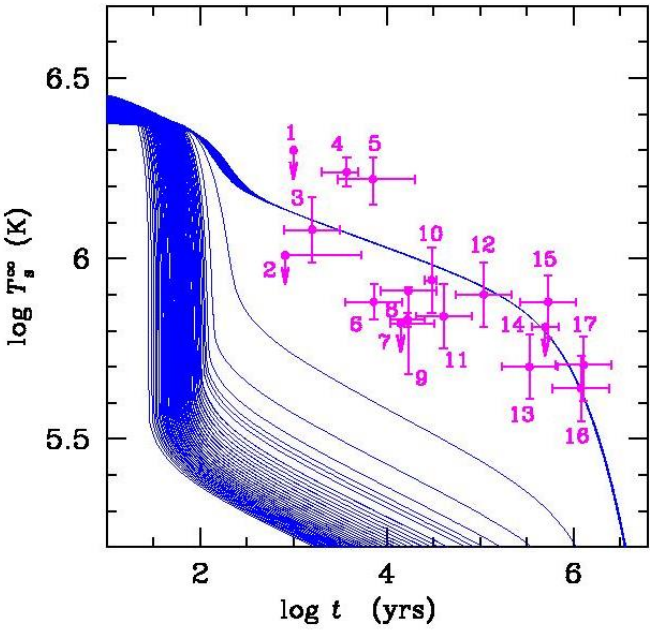
Neutrino emission. Effects of Pairing.

Two main effects

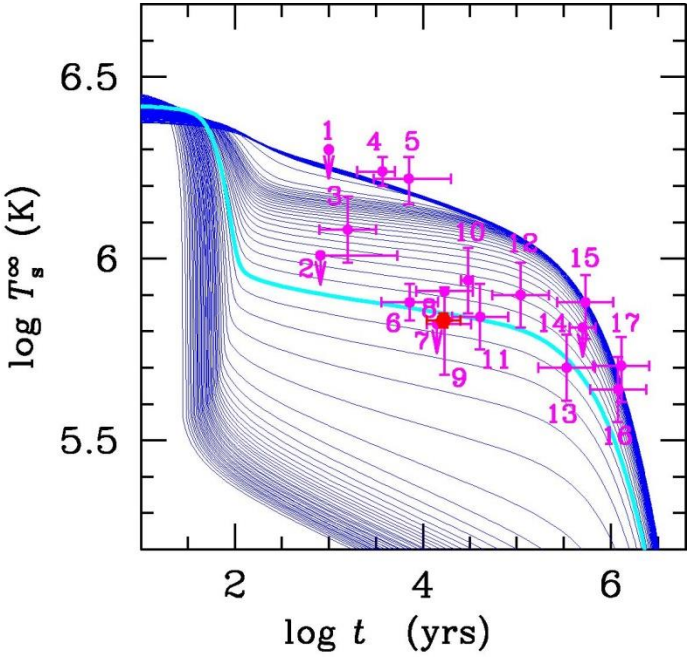
I. Damping of the traditional neutrino emission processes

$$L_\nu \to L_\nu \times \exp\left(-\alpha T_c/T\right), \quad T \ll T_c$$

no pairing: sharp Durca transition



with pairing: gradual transition



From $1.1M_\odot$ to $1.9M_\odot$ with step $0.01M_\odot$

Cooper pair formation emission

Two main effects

II. New channel of neutrino emission due to Cooper pairing

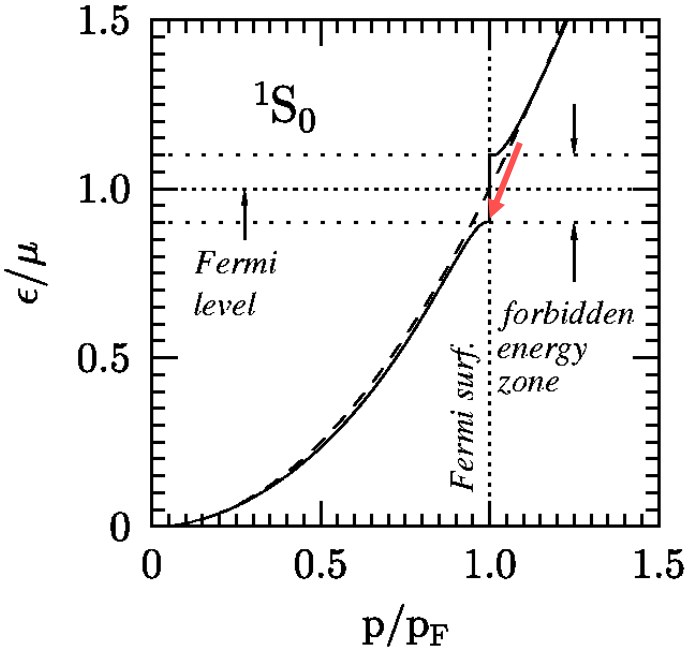
$$\tilde{N} + \tilde{N} \to \nu + \bar{\nu}$$

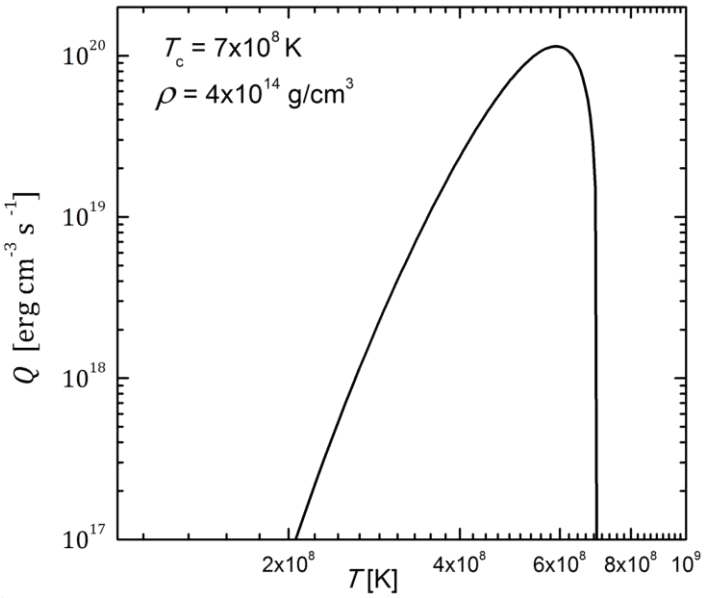
Flowers, Ruderman and Sutherland (1976)

neutral current counterpart to DUrca

$$Q_0^{(\mathrm{CP})} = 1.17 \times 10^{21} \frac{m_{\mathrm{n}}^*}{m_{\mathrm{n}}} \frac{p_{\mathrm{Fn}}}{m_{\mathrm{n}} c} T_9^7 \mathcal{N}_\nu R\left(\frac{\Delta}{T}\right) \frac{\mathrm{erg}}{\mathrm{cm}^3\ \mathrm{s}}$$

CPF emissivity



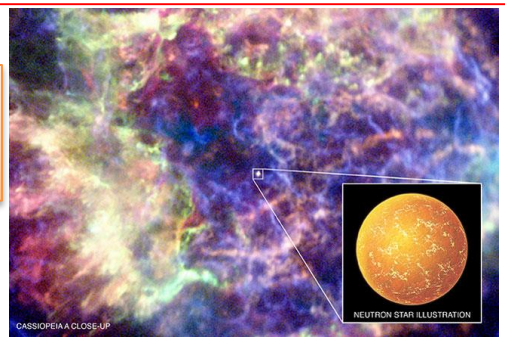


Maximal at $T \sim 0.7 T_c$

Astro: NS in SNR Cassiopeia A

Possible fast cooling of 330 yr old star

Page et al., 2011
Shternin et al., 2011



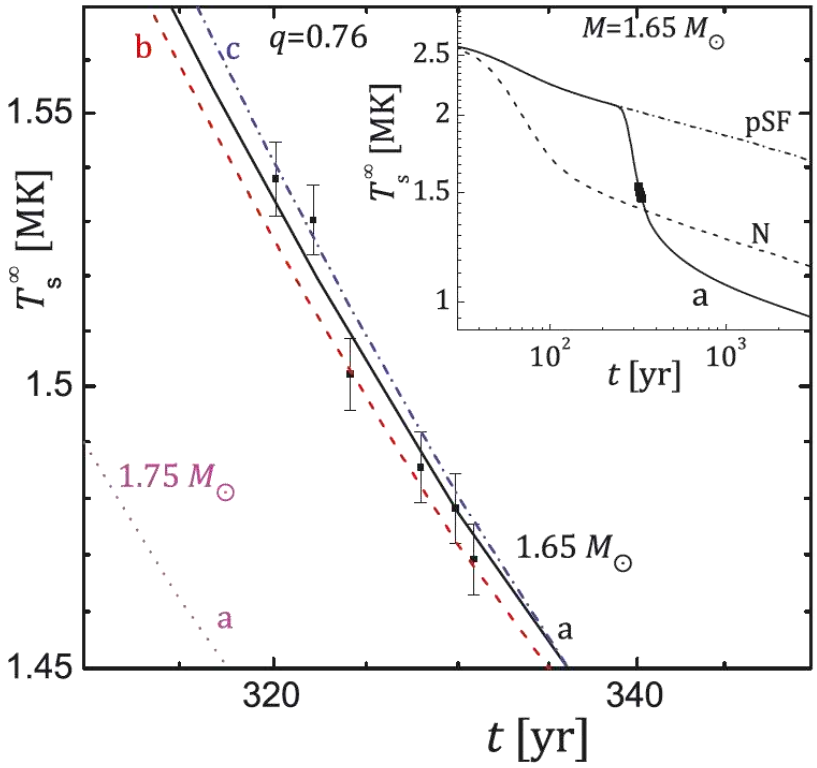
Latest data (Wijngaarden+19)

$$2.2\% - 2.7\% \text{ by } 10 \text{ yr}$$

Explained by the resent splash of CPF neutrinos on the background of slow (pSC-suppressed) cooling

In this model one can constrain the properties of superfluidity inside the star

$$\widetilde{T}_{\rm cnmax} \approx (3-6)\times 10^8 \text{ K}$$



Part III: Bulk viscosity

Bulk viscosity

In Fermi liquid, there is a bulk viscosity from collisions, but it is small
The dissipation in bulk viscosity form comes from chemical equilibration

Mandelshtam and Leontovich 1937

Bulk viscosity $\zeta(\omega)$ = dissipative response to compression and expansion $(\nabla \boldsymbol{v} \propto \dot{V})$

$$V(t) = V_0 + \delta V \cos \omega t$$

$$\zeta(\omega) = 2\langle \dot{E} \rangle \left(\frac{V_0}{\delta V} \right)^2 \frac{1}{\omega^2}$$

With the dissipated power in an oscillator period $\tau = 2\pi/\omega$

$$\langle \dot{E} \rangle = -\frac{1}{\tau V_0} \int_0^\tau dt P(t) \frac{dV}{dt} = \frac{B}{C} \gamma \langle \delta\mu(t) \delta V(t) \rangle$$

B, C – certain susceptibilities in equilibrium

species production in reactions $\Delta\Gamma = \lambda \delta\mu = \gamma \delta\mu / C$

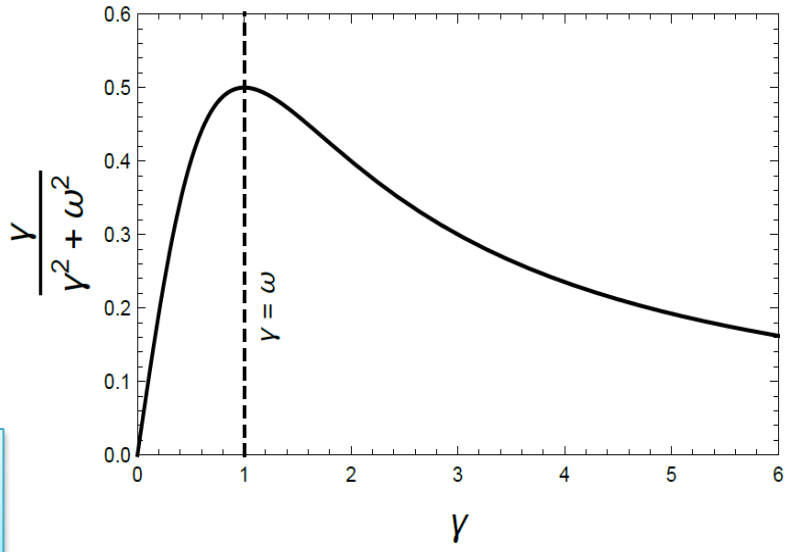
Result $\zeta(\omega) = \frac{B^2}{C} \frac{\gamma}{\gamma^2 + \omega^2}$

Bulk viscosity

Bulk viscosity is resonance phenomena

$$\zeta(\omega) = \frac{B^2}{C}\frac{\gamma}{\gamma^2+\omega^2}$$

It is maximal for $\gamma = \omega$



Need microscopic rate γ to be of the order of star oscillations (a case of weak reactions)

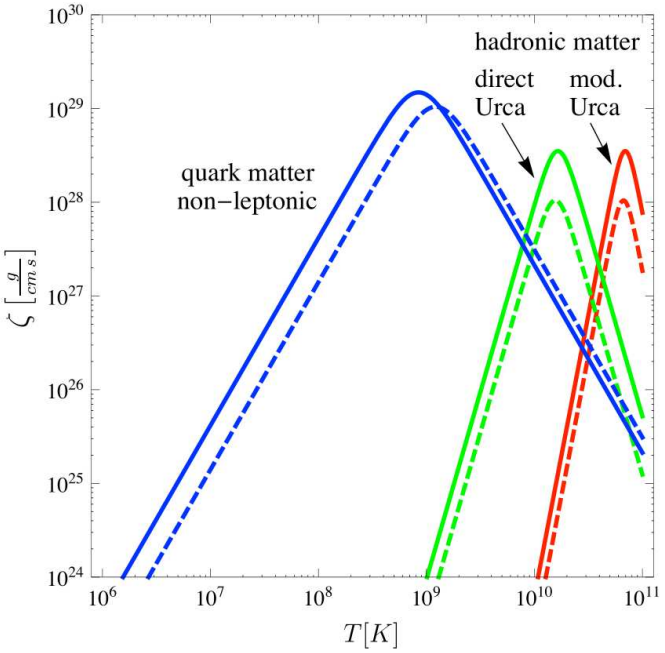
$\gamma = \lambda C$ typically monotonically increases with T hence there is a maximum of ζ at a certain T

Bulk viscosity

hadronic matter	quark matter
direct Urca, $p + e \to n + \nu_e$ **modified Urca**	**non-leptonic process** $u + d \leftrightarrow u + s$
hyperons, e.g.: $n + n \leftrightarrow p + \Sigma^-$	Urca: $u + e \to d + \nu_e$
nn, pp pairing: rates suppressed	CFL: $K^0 \leftrightarrow \phi + \phi$

For non-leptonic processes: larger phase space

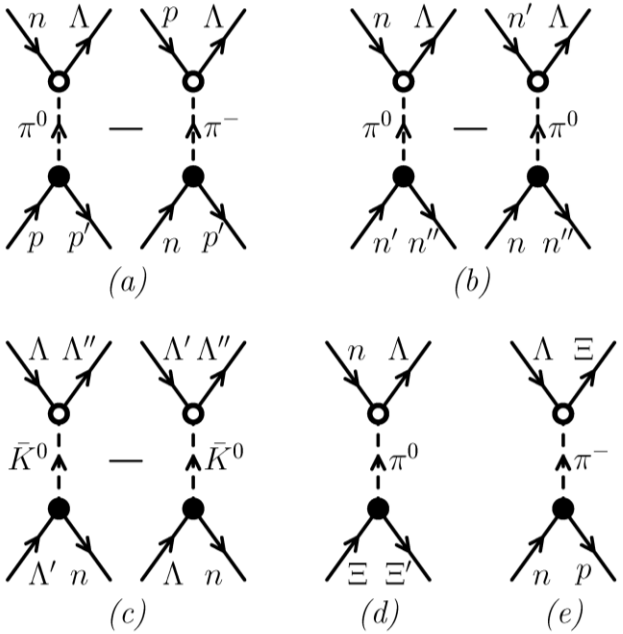
Uncertainties from strong interactions in susceptibilities and reaction rates



M.G. Alford, et al., J. Phys. G 37, 125202 (2010)

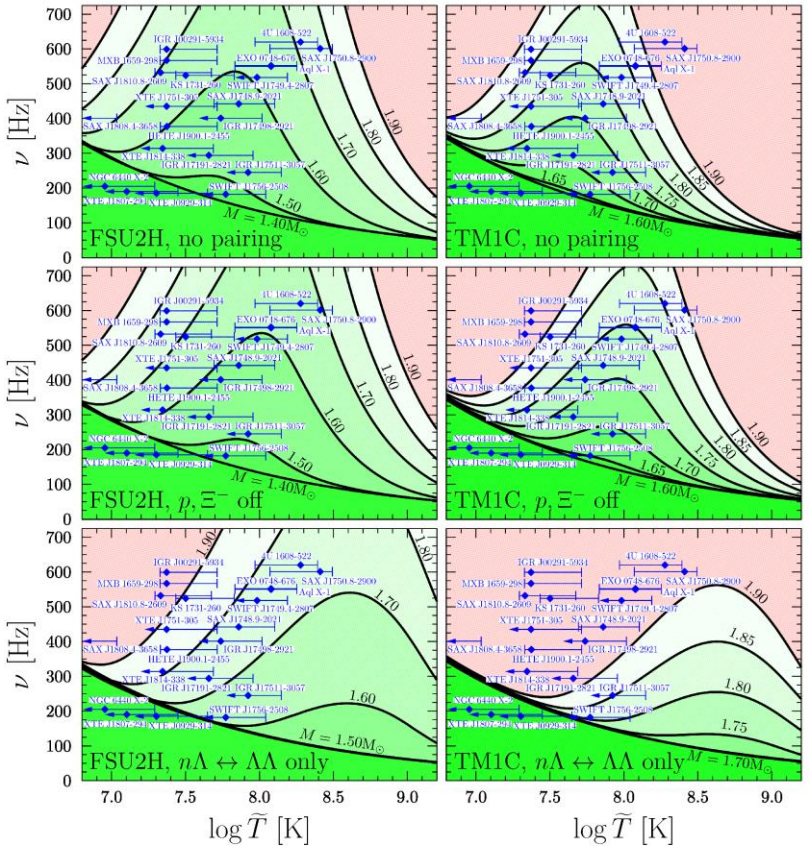
Bulk viscosity

Non-leptonic reactions in hyperon matter



D.D. Ofengeim et al., PRD 100, 103017 (2019)

Stability windows



Conclusion remarks

- Transport properties of NS matter is a rich field with many open problems in theory and in connection with observations. We discussed few examples.
- there can be various phases of matter that have very distinct transport properties.
- uncertain microphysical input from the strong interaction sector
- non-ideal Coulomb mixtures (even single-species around melting point), anisotropic transport in pasta phases
- transport in superfluid phases
- dissipation at high-T case (NS mergers) – emerging part of the field
- exotic processes, e.g. axion emission
- all above with magnetic field
- and more

Physics of Neutron Stars – 2020
in St. Petersburg
July 20 – July 24, 2020
Register before March 16
http://www.ioffe.ru/astro/NS2020/



Thank you for attention!